Chapter 1
Stabilization control of power system models

In this Chapter, we will explain frequency stabilization control and transient stabilization control of power system models. The structure of this chapter is as follows. First, in Section 1, we outline the automatic generation control, which is a representative example of frequency stabilization control, to suppress the deviation of angular frequency caused by load variations, and confirm through numerical simulations that the steady-state power flow state changes by adjusting the parameters of the controller. Next, in Section 2, as an advanced topic, we perform mathematical stability analysis of frequency stabilization control. In particular, based on passivity that does not depend on equilibrium points for nonlinear systems, we show the relationship between the stability region of the power system model and the convex region of potential energy function. Furthermore, in Section 3, we explain the configuration and functions of standard automatic voltage regulators and power system stabilizers used for transient stabilization control. Finally, in Section 4, as an advanced topic, we explain the design methodology of power system stabilizers based on retrofit control theory.

1 Frequency stabilization control

1.1 Automatic generation control using broadcast-type PI controller

1.1.1 Overview of Automatic Generation Control

In this section, we will explain the principle of **Automatic Generation Control (AGC)** which adjusts the generation output appropriately in response to unknown load variations. Automatic Generation Control adjusts the generation output by performing control actions such as increasing the generation output when the power supply is insufficient compared to the demand, and decreasing the generation output when the power supply is excessive, based on the observed frequency devia-

tions of multiple generators. This control action is based on the general characteristic of power systems that negative frequency deviations occur when the power supply is insufficient compared to the demand, and positive frequency deviations occur when the power supply is excessive. In power system engineering, the overall control to asymptotically converge the frequency deviation to zero is generally referred to as **Frequency Stabilization Control**. Automatic Generation Control is one of the methods for Frequency Stabilization Control.

In actual power system operation, the central dispatch center performs Automatic Generation Control. Although the basic operating principle is common, there are several methods depending on the objectives. The target is to maintain the frequency within a range of about ±0.2Hz with respect to the reference frequency of 50Hz or 60Hz. Note that the frequency deviation of the voltage phasor at a nearby substation is often observed instead of the frequency deviation of the generator, because the frequency of the voltage phasor at the substation is generally close to that of the generator. Also, one of the challenges of Automatic Generation Control is that there are many unknown constants and variables in the actual power system. For example, it is possible to roughly predict the total amount of load in a time scale of about 30 minutes, but it is not possible to accurately grasp the values of individual loads that change every moment. It is also difficult to accurately know all the constants such as the impedance of each transmission line. Therefore, it is necessary to design control algorithms that can be applied without knowing the accurate model of the entire power system. In actual power system operation, weather forecast information, temperature data, historical data, and other information are used to predict changes in total demand for certain areas to some extent. The size of the area and the method used vary, but it is impossible to predict the demand completely.

On the other hand, as confirmed in the numerical examples in Section **??**, when the supply-demand balance is not maintained, various problems such as frequency deviation and tie-line power flow deviation may occur. Therefore, it is important to establish an effective Automatic Generation Control method that can mitigate the impact of unknown load variations and maintain the stability of the power system. In this section, we will explain the principle of Automatic Generation Control using a broadcast-type PI controller, which is one of the methods for Frequency Stabilization Control. Therefore, it is necessary to design a control algorithm that can be applied without knowing the accurate model of the entire power system. In actual power system operation, weather forecast information, temperature data, historical data, and other information are used to predict changes in total demand for certain areas to some extent. The size of the area and the method used vary, but it is impossible to predict the demand completely.

1.1.2 Formulation of automatic generation control

In the following, we consider a generator model with the bus voltage phasor as the input, as discussed in Section **??**. The dynamic characteristics of the generator are restated as follows:

$$\begin{aligned}
\dot{\delta}_i &= \omega_0 \Delta\omega_i \\
M_i \Delta\dot{\omega}_i &= -D_i \Delta\omega_i - P_i + P_{\text{mech}i} \\
\tau_i \dot{E}_i &= -\tfrac{X_i}{X_i'} E_i + \left(\tfrac{X_i}{X_i'} - 1\right) |\boldsymbol{V}_i| \cos(\delta_i - \angle \boldsymbol{V}_i) + V_{\text{field}i}
\end{aligned} \tag{1a}$$

When considering active power and reactive power as outputs, we have:

$$\begin{aligned}
P_i &= \frac{E_i |\boldsymbol{V}_i|}{X_i'} \sin(\delta_i - \angle \boldsymbol{V}_i), \\
Q_i &= \frac{E_i |\boldsymbol{V}_i|}{X_i'} \cos(\delta_i - \angle \boldsymbol{V}_i) - \frac{|\boldsymbol{V}_i|^2}{X_i'}
\end{aligned} \tag{1b}$$

According to this expression, the load model for inputting the phase of the bus-bar voltage and outputting the active and reactive powers is also shown again. The constant impedance model is given by:

$$P_i = -\frac{|\boldsymbol{V}_i|^2}{\text{Re}\left[\overline{z}^{\star}_{\text{load}i}\right]}, \qquad Q_i = -\frac{|\boldsymbol{V}_i|^2}{\text{i}\left[\overline{z}^{\star}_{\text{load}i}\right]} \tag{2a}$$

where $z^{\star}_{\text{load}i}$ is a constant representing the impedance of the load.

Similarly, the constant current model is expressed as:

$$P_i = |\boldsymbol{V}_i| \,\text{Re}\left[\boldsymbol{I}^{\star}_{\text{load}i}\right], \qquad Q_i = -|\boldsymbol{V}_i| \text{i}\left[\boldsymbol{I}^{\star}_{\text{load}i}\right] \tag{2b}$$

where $\boldsymbol{I}^{\star}_{\text{load}i}$ is a constant representing the current phase of the load.

The constant power model is given by:

$$P_i = P^{\star}_{\text{load}i}, \qquad Q_i = Q^{\star}_{\text{load}i} \tag{2c}$$

where $P^{\star}_{\text{load}i}$ and $Q^{\star}_{\text{load}i}$ are constants.

These generator models and load models are combined to describe the entire power system using a differential-algebraic equation (DAE) model, as shown in the algebraic equation system:

$$\begin{aligned}
P_1 + \boldsymbol{j} Q_1 &= \sum_{j=1}^{N} \overline{\boldsymbol{Y}}_{1j} |\boldsymbol{V}_1| |\boldsymbol{V}_j| e^{\boldsymbol{j}(\angle \boldsymbol{V}_1 - \angle \boldsymbol{V}_j)} \\
&\vdots \\
P_N + \boldsymbol{j} Q_N &= \sum_{j=1}^{N} \overline{\boldsymbol{Y}}_{Nj} |\boldsymbol{V}_N| |\boldsymbol{V}_j| e^{\boldsymbol{j}(\angle \boldsymbol{V}_N - \angle \boldsymbol{V}_j)}
\end{aligned} \tag{3}$$

where the generator bus indices are denoted by the set $\mathcal{I}\text{G}$ and the load bus indices are denoted by the set $\mathcal{I}\text{L}$, and without loss of generality, we can define:

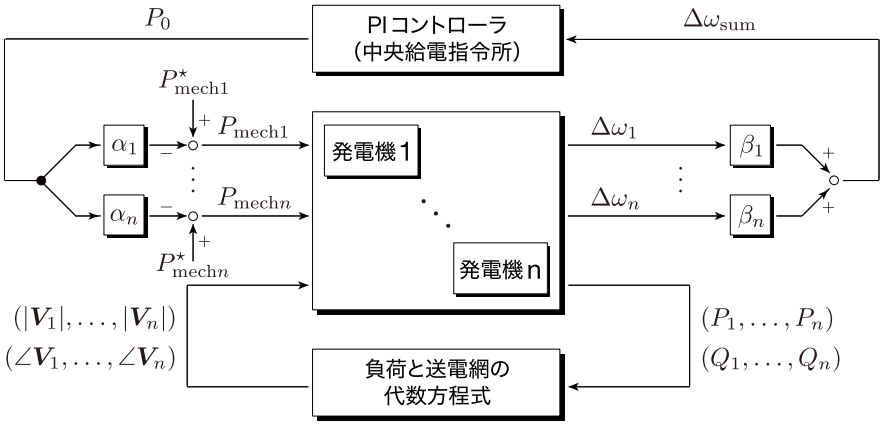

Fig. 1 Signal transmission structure for automatic power generation control

$$\mathcal{I}_{\mathrm{G}} := \{1,\ldots,n\}, \qquad \mathcal{I}_{\mathrm{L}} := \{n+1,\ldots,n+m\}$$

where n represents the total number of generator buses and m represents the total number of load buses. Furthermore, N represents the total number of buses, which is equal to $n+m$.

The automatic generation control (AGC) is a control algorithm that adjusts the mechanical input $P_{\mathrm{mech}i}$ in Equation (1). Here, we consider a broadcast-type PI controller that observes the weighted sum of frequency deviations for all generators and sends a control input with appropriate weighting to all generators. Specifically, for each $i \in \mathcal{I}_{\mathrm{G}}$, we set:

$$P_{\mathrm{mech}i}(t) = P^{\star}_{\mathrm{mech}i} - \alpha_i \underbrace{\left\{ k_{\mathrm{P}} \Delta\omega_{\mathrm{sum}}(t) + k_{\mathrm{I}} \int_0^t \Delta\omega_{\mathrm{sum}}(\tau)\, d\tau \right\}}_{P_0(t)} \tag{4a}$$

where $P^{\star}_{\mathrm{mech}i}$ is a constant representing the standard setting value of the mechanical input. Moreover, α_i is a non-negative constant specifying the contribution of generator i, and:

$$\Delta\omega_{\mathrm{sum}}(t) := \sum_{i=1}^{n} \beta_i \Delta\omega_i(t)$$

is the weighted sum of frequency deviations with non-negative weights β_i. Furthermore, k_{P} and k_{I} are positive constants representing the gains of the PI controller. This AGC controller has a structure where the generated signal $P_0(t)$, which is produced by a single PI controller with weighting of α_i and β_i, is simultaneously broadcasted to all generators (Figure 1). Note that Equation 4a can be expressed as a differential equation as follows:

$$\begin{aligned} \dot{\xi} &= \Delta\omega_{\mathrm{sum}} \\ P_{\mathrm{mech}i} &= P^{\star}_{\mathrm{mech}i} - \alpha_i \left(k_{\mathrm{P}}\Delta\omega_{\mathrm{sum}} + k_{\mathrm{I}}\xi\right) \end{aligned} \tag{4b}$$

In electric power systems engineering, the non-negative constant α_i is referred to as the **participation factor** of generator i. It should be noted that in real-world thermal power generation and nuclear power generation, there is a **prime mover** that generates mechanical input by rotating a turbine using high-pressure steam generated by thermal or nuclear power. The prime mover incorporates a **governor** that automatically controls the rotation speed of the generator. In order to analyze more realistic automatic generation control, it is necessary to consider a prime mover model that takes input from the central dispatch center as setpoint and outputs mechanical input to the generator [**?**, Chapter 3].

By changing the ratio of participation factors, it is possible to adjust the values of effective power supplied by each generator in a balanced steady-state load flow condition. From the perspective of system control engineering, this can be interpreted as "moving the stable equilibrium point of the power system model by switching controllers." As analyzed in Chapter **??**, the stability of the power system depends on the choice of equilibrium point. The total generation cost and transmission loss of the power system also depend on the choice of equilibrium point. Therefore, appropriately switching the participation factors according to the distribution of load can lead to improved system stability and reduced economic costs.

In actual power system operation, the updating of participation factors is typically done at intervals of several minutes to several tens of minutes [**?**, Section 11.1]. In the terminology of power system engineering, the scheme for updating these participation factors is called **economic load dispatching control** (EDC). The control algorithm that uses the participation factors as constants during the updating interval is called **load frequency control** (LFC). However, it should be noted that there may be cases where there is no clear distinction between economic load dispatching control and load frequency control in the literature, or where economic load dispatching control is considered as a different scheme, so caution is necessary.

1.2 Numerical simulation of frequency stabilization control

Let's verify the effectiveness of frequency stabilization control using a simple example.

Example 1.1 Frequency stabilization by Automatic Generation Control Consider the power system model consisting of 3 busbars as discussed in Examples **??**, **??**, and **??**. The physical constants of the generators and transmission lines are set to the same values as in Example **??**, and the initial values of the internal states of the generators are set to the steady-state values shown in Table **??**. In addition, the field input is assumed to be constant at the values shown in Table **??**.

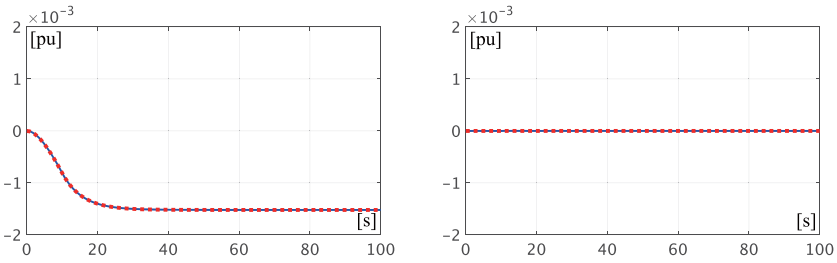

(a) No automatic power generation control (b) With automatic power generation control

Fig. 2 Time response of angular frequency deviation to power consumption increase
(Blue solid line: $Delta\omega_1$, Red dashed line: $Delta\omega_3$)

The load at busbar 2 is set to a constant power model, and we consider a case where the consumption of active power increases by 1% from the initial steady-state load flow condition. First, we show the time response of the frequency deviation when there is no automatic generation control and the mechanical input of the generators is constant at the values shown in Table **??**, as shown in Figure 2(a). It can be seen that the steady-state value of the frequency deviation does not become zero because the supply and demand are not balanced due to the increased power consumption by the load.

Next, we show the results when the broadcast-type PI controller of Equation 4 is incorporated as automatic generation control, with the parameters of the controller set to the values shown in Table 1(a), as shown in Figure 2(b). From this figure, it can be seen that the frequency deviation hardly occurs even when the consumption of load power changes, due to the effectiveness of automatic generation control.

Table 1 Controller Parameter Setting

Setup	k_P	k_I	α_1	α_3	β_1	β_3
(a)	100	500	1	3	1	3
(b)	100	500	1	1	1	1
(c)	100	500	3	1	3	1

Next, let us confirm the change in steady-state power flow conditions by adjusting the contribution coefficients of the broadcast-type PI controller in Equation 4 to achieve supply-demand balance.

Example 1.2 Change in steady-state power flow conditions by adjusting contribution coefficients Consider a power system model consisting of two generators and one load, similar to Example 1.1. Here, we confirm that the ratio of active power

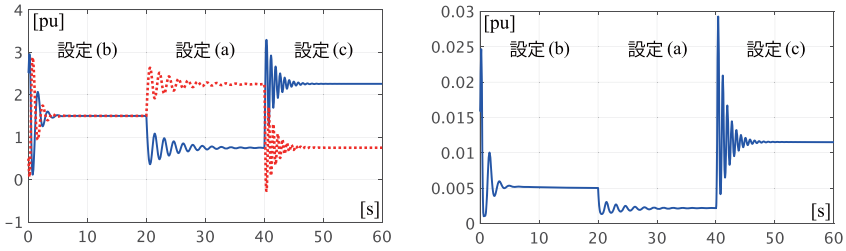

(a) Blue solid line: P_1, Red dashed line: P_3.

(b) Transmission loss $P_1 + P_2 + P_3$.

Fig. 3 Time response of effective power to changes in contribution factor

supplied by Generator 1 and Generator 3 changes by varying the contribution coefficients of the broadcast-type PI controller in Equation 4. Specifically, we switch the contribution coefficients as follows:

- Parameters of 1 (b) are set for 0 [s] to 20 [s].
- Parameters of 1 (a) are set for 20 [s] to 40 [s].
- Parameters of 1 (c) are set for 40 [s] to 60 [s].

The resulting time response is shown in Figure 3(a). The solid blue line represents the value of active power supplied by Generator 1 (P_1), and the dashed red line represents the value of active power supplied by Generator 3 (P_3). From this result, it can be seen that the ratio of P_1 and P_3 in the steady-state power flow conditions matches the ratio of contribution coefficients α_1 and α_3.

Next, the time response of the total active power transmission loss $P_1 + P_2 + P_3$, which represents the power transmission loss due to active power, is shown in Figure 3(b). Note that P_2 is the active power consumed by the load and its value is constant at -3.

From this figure, it can be seen that the magnitude of active power transmission loss varies depending on the realized steady-state power flow conditions. In particular, when the parameters of the broadcast-type PI controller are set to the values in Table 1 (a), i.e., when power is mainly supplied using the lossless transmission line between Bus 2 and Bus 3, the total power transmission loss of the entire power system is smaller, which is consistent with the discussion in Example **??**. The admittance of the transmission lines is set to the values in Equation (**??**).

As shown in Example 1.2, by adjusting the contribution coefficients of a broadcast-type PI controller, it is possible to change the steady-state power flow condition. At the same time, the magnitude of transmission losses and the required generation cost for each steady-state power flow condition also change. Therefore, by appropriately controlling the contribution coefficients, it is possible to achieve more economical system operation. However, it should be noted that a steady-state power flow condition with lower economic costs is not necessarily a highly stable equilibrium point,

so it is important to carefully consider trade-offs between economic efficiency and stability.

2 Mathematical stability analysis of frequency stabilization control system

2.1 Power system model under consideration

2.1.1 Assumptions on Power System Model and Automatic Generation Control

In Section **??**, an approximate linear model was derived under the assumption that the power system model is in the vicinity of steady-state power flow conditions, and necessary and sufficient conditions for steady-state stability were analyzed. In this section, using the concept of passivity for nonlinear systems, we analyze the frequency stability of the power system model described as a system of differential-algebraic equations, taking into consideration the stability of the entire feedback control system with automatic generation control. Specifically, we conduct stability analysis under the following assumptions.

- All generators are expressed with the generator model of Equation (2). However, it is assumed that the field voltage of each generator is set to a constant.
- All loads are expressed with the constant power model of Equation 2c.
- For algebraic equations for the power grid of Equation 3, conductance of all transmission lines is assumed to be 0.
- For the broadcast-type PI controller of Equation (4), automatic generation control is performed. However, it is assumed that α_i and β_i are equal for all $i \in \mathcal{I}_{\mathrm{G}}$ for the weight of the participation factor and frequency deviation.

The first and second assumptions refer to considering a standard model for the generator and load in the power system. The third assumption regarding the transmission network implies that transmission losses are assumed to be zero, which is essential for conducting stability analysis mathematically. In reality, it is not possible to completely eliminate transmission losses in a power system, but reducing transmission losses can be achieved by transmitting power at higher voltages with lower currents. The discussion in this section assumes that transmission losses can be approximately considered as zero due to high-voltage transmission. The fourth assumption is necessary for the input-output characteristics of the broadcast-type PI controller to be passive. However, it should be noted that even if some coefficients are zero, as long as at least one contribution coefficient α_i for $i \in \mathcal{I}_{\mathrm{G}}$ is positive, it is acceptable.

Furthermore, as shown in the analysis of Section **??**:

- The frequency deviation of all generators become equalize under a steady power flow distribution.

The following frequency stability analysis is based on this fact. Specifically, in order for the integral controller in the broadcast-type PI controller to make the steady-state angular frequency deviations of all generators zero, it is necessary for the above-mentioned angular frequency deviations to automatically synchronize with each other. Note that this requires the characteristic of automatic synchronization among the angular frequency deviations using only one integrator included in the broadcast-type PI controller.

2.1.2 Representation of power system with automatic generation control as a feedback system

Similar to the discussion in Section **??**, we consider representing the power system model as a feedback system consisting of two subsystems. The first subsystem is described by the following equations:

$$\mathbb{F}: \begin{aligned} M\Delta\dot{\omega} &= -D\Delta\omega + u_{\mathbb{F}} + P^{\star}_{\text{mech}} \\ y_{\mathbb{F}} &= \omega_0 \Delta\omega \end{aligned} \tag{5}$$

However, $\Delta\omega$ is a vector composed of $\Delta\omega_i$ stacked vertically, and M and D are matrices formed by diagonally arranging M_i and D_i. Also, $P^{\star}_{\text{mech}}$ is a constant vector composed of $P^{\star}_{\text{mech}i}$. This $\mathbb{F}$ is equivalent to the mechanical subsystem in Section **??**, except for the difference in the constant vector $P^{\star}_{\text{mech}}$. The second subsystem is represented by the nonlinear differential-algebraic equation system of the electrical subsystem in Section **??**, given by:

$$\mathbb{G}_i: \begin{aligned} \dot{\delta}_i &= u_{\mathbb{G}_i} \\ \tau_i \dot{E}_i &= -\tfrac{X_i}{X_i'} E_i + \left(\tfrac{X_i}{X_i'} - 1\right) |\boldsymbol{V}_i| \cos(\delta_i - \angle \boldsymbol{V}_i) + V^{\star}_{\text{field}i} \\ y_{\mathbb{G}_i} &= \tfrac{E_i |\boldsymbol{V}_i|}{X_i'} \sin(\delta_i - \angle \boldsymbol{V}_i) \end{aligned} \tag{6a}$$

The voltage phasor of the bus in Equation 6a satisfies a set of simultaneous equations for all generator buses as follows:

$$\begin{aligned} P_i &= \sum_{j=1}^{N} B_{ij} |\boldsymbol{V}_i| |\boldsymbol{V}_j| \sin(\angle \boldsymbol{V}_i - \angle \boldsymbol{V}_j) \\ Q_i &= -\sum_{j=1}^{N} B_{ij} |\boldsymbol{V}_i| |\boldsymbol{V}_j| \cos(\angle \boldsymbol{V}_i - \angle \boldsymbol{V}_j) \end{aligned} \qquad i \in \mathcal{I}_{\text{G}} \tag{6b}$$

and a set of coupled equations for all load bus bars given by:

$$\begin{cases} P^{\star}_{\mathrm{load}i} = \displaystyle\sum_{j=1}^{N} B_{ij}|\boldsymbol{V}_i||\boldsymbol{V}_j|\sin(\angle\boldsymbol{V}_i - \angle\boldsymbol{V}_j) \\ Q^{\star}_{\mathrm{load}i} = -\displaystyle\sum_{j=1}^{N} B_{ij}|\boldsymbol{V}_i||\boldsymbol{V}_j|\cos(\angle\boldsymbol{V}_i - \angle\boldsymbol{V}_j) \end{cases} \qquad i \in \mathcal{I}_{\mathrm{L}} \tag{6c}$$

In addition, the active power P_i and reactive power Q_i in Equation (6b) are defined by Equation (1b). Also, B_{ij} represents the (i, j) element of the susceptance matrix B, which is the imaginary part of the admittance matrix $\boldsymbol{Y}$. In the following, we consider the combination of Equations (6a) to (6c) for all generator buses $i \in \mathcal{I}_{\mathrm{G}}$ as one subsystem, and denote it as the electrical subsystem $\mathbb{G}$.

Furthermore, the dynamic characteristics of the broadcast-type PI controller in Equation (4) are represented as follows:

$$\mathbb{K} : \begin{cases} \dot{\xi} = h^{\mathsf{T}} u_{\mathbb{K}} \\ y_{\mathbb{K}} = h\left(k_{\mathrm{P}} h^{\mathsf{T}} u_{\mathbb{K}} + k_{\mathrm{I}}\xi\right) \end{cases} \tag{7}$$

where h is a column vector consisting of α_i.

In this case, the inputs and outputs of the aforementioned subsystems $\mathbb{F}$, $\mathbb{G}$, and controller $\mathbb{K}$ are interconnected as follows:

$$u_{\mathbb{F}} = -y_{\mathbb{K}} + v_{\mathbb{F}}, \qquad u_{\mathbb{K}} = \frac{1}{\omega_0} y_{\mathbb{F}} \tag{8a}$$

$$u_{\mathbb{G}} = y_{\mathbb{F}}, \qquad v_{\mathbb{F}} = -y_{\mathbb{G}} \tag{8b}$$

This represents the entire feedback control system incorporating automatic generation control. However, it should be noted that the ”power balance equation” block includes unknown model parameters such as load consumption power and transmission line admittance. The block diagram of the entire feedback control system is shown in Figure 4. Please note that the block representing the ”power balance equation” includes unknown model parameters such as load consumption power and transmission line admittance.

2.2 Equilibrium-independent passivity of power system models

2.2.1 Equilibrium-independent passivity

The discussion in Section **??** was based on an approximate linear model, and the convergence to zero of the internal state represented the asymptotic convergence to a specific steady-state power flow condition in the original nonlinear model. On the other hand, in power system models represented as nonlinear differential-algebraic equation systems, the internal state does not necessarily converge to zero even at steady-state power flow conditions where power supply and demand are balanced.

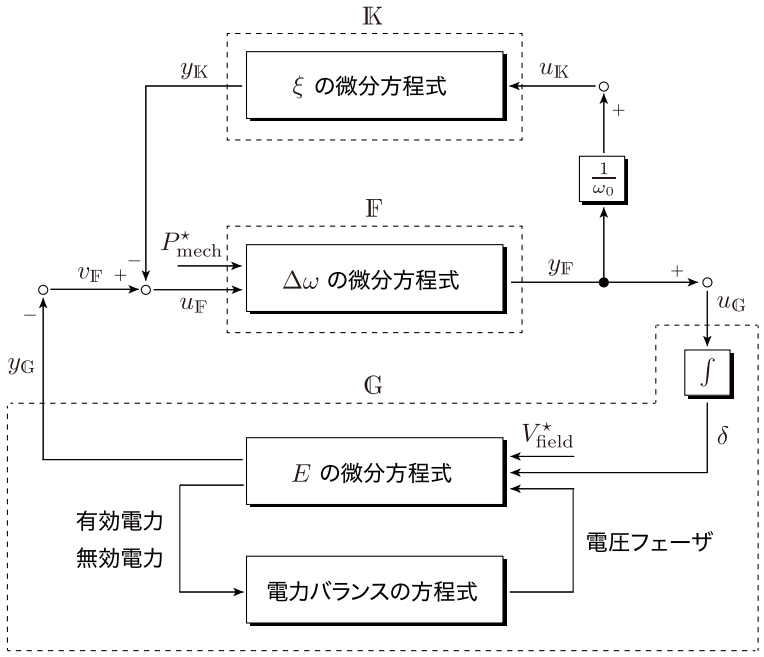

Fig. 4 Feedback control system incorporating automatic power generation control

Furthermore, the steady-state power flow condition itself can change depending on set values such as mechanical inputs. Therefore, it is desirable to conduct stability analysis that does not depend on the selection of individual steady-state power flow conditions (equilibrium points). A concept proposed in control engineering for such analysis is called **equilibrium-independent passivity** [**?**, **?**]. Note that in some literature, it is also referred to as **shifted passivity** [**?**]. Its definition is given as follows.

Definition 1.1 (Equilibrium-independent passivity) Let us consider a nonlinear system:

$$\Sigma : \begin{cases} E\dot{x} = f(x) + Bu + Rd^{\star} \\ \quad y = h(x) \end{cases} \tag{9}$$

where $f : \mathcal{X} \to \mathbb{R}^n$ and $h : \mathcal{X} \to \mathbb{R}^m$ are smooth functions, and $B \in \mathbb{R}^{n\times m}$, $E \in \mathbb{R}^{n\times n}$, $R \in \mathbb{R}^{n\times p}$ are matrices. Also, $d^{\star} \in \mathbb{R}^p$ is a constant vector. Here, $\mathcal{X}$ represents the admissible state space.

The set of achievable equilibrium points by constant inputs is denoted as:

$$\mathcal{E}_{\Sigma} := \left\{ x^{\star} \in \mathcal{X} : \text{there exists } u^{\star} \text{ satisfying } 0 = f(x^{\star}) + Bu^{\star} + Rd^{\star} \right\}$$

For each equilibrium point $x^\star \in \mathcal{E}\Sigma$, if there exists a differentiable positive semi-definite function $Wx^\star : \mathcal{X} \to \mathbb{R}\geq 0$ such that $Wx^\star(x^\star) = 0$ and for any input u, the following inequality holds for all $t \geq 0$:

$$\frac{d}{dt}W_{x^\star}\big(x(t)\big) \leq \big(u(t) - u^\star\big)^\mathsf{T}\big(y(t) - y^\star\big), \qquad \forall t \geq 0$$

then Σ is called **equilibrium-independent passive**. Here, $u^\star$ and $y^\star$ denote the steady-state input and output at the equilibrium point, respectively, and are defined as:

$$u^\star := -(B^\mathsf{T}B)^{-1}B^\mathsf{T}\big\{f(x^\star) + Rd^\star\big\}, \qquad y^\star := h(x^\star)$$

In particular, if there exists a positive constant ρ such that the following inequality holds for all $t \geq 0$:

$$\frac{d}{dt}W_{x^\star}\big(x(t)\big) \leq \big(u(t) - u^\star\big)^\mathsf{T}\big(y(t) - y^\star\big) - \rho\big\|y(t) - y^\star\big\|^2, \qquad \forall t \geq 0$$

then Σ is called **equilibrium-independent strictly passive**.

In Definition 1.1, the passivity of the system is defined with respect to the equilibrium point $x^\star \in \mathcal{E}\Sigma$ as a reference. In the context of linear systems, it is known that this definition of passivity is equivalent to the definition of passivity in Section **??**, unless the system has a zero eigenvalue [**?**]. Note that the function $W_{x^\star}(x)$ mentioned above is called the storage function, similar to conventional passivity definitions. It should be noted that this storage function $W_{x^\star}(x)$ is an implicit function of the equilibrium point $x^\star$.

COFFEE BREAK

Descriptor representation: The matrix E in Equation 9 is introduced to represent the electrical subsystem $\mathbb{G}$ of the differential-algebraic equation system given by Equation (6). Specifically, by setting:

$$E = \begin{bmatrix} I & 0 \\ 0 & 0 \end{bmatrix}$$

the system Σ in Equation 9 represents the following differential-algebraic equation system:

$$\begin{cases} \dot{x}_1 = f_1(x_1, x_2) + B_1 u + R_1 d^\star \\ 0 = f_2(x_1, x_2) \\ y = h(x_1, x_2) \end{cases}$$

When applied to the electrical subsystem $\mathbb{G}$, x_1 is a vector containing all δ_i and E_i, and x_2 is a vector containing all $|\boldsymbol{V}_i|$ and $\angle \boldsymbol{V}_i$. On the other hand, when

E is regular, it represents a differential equation system like the mechanical subsystem $\mathbb{F}$ given by Equation 5. This type of system representation is called the **descriptor representation**.

In reference [**?**], it is shown that when a system is passive regardless of its equilibrium point, its storage function can be expressed in the form of Equation 10 using a certain function $U(x)$:

$$W_{x^\star}(x) = U(x) - U(x^\star) - \nabla U^\mathsf{T}(x^\star)(x - x^\star) \tag{10}$$

In Definition 1.1, it is a requirement that the storage function $W_{x^\star}(x)$ in Equation 10 is a positive semi-definite function. Specifically, the condition is that Equation 11 holds:

$$U(x) \geq U(x^\star) + \nabla U^\mathsf{T}(x^\star)(x - x^\star) \tag{11}$$

If this inequality holds for any pair $(x, x^\star) \in \mathcal{X}\times\mathcal{X}$, then for each equilibrium point $x^\star \in \mathcal{E}\Sigma$, $Wx^\star(x)$ is a positive semi-definite function. The inequality in Equation 11 expresses the convexity of the function $U(x)$. As will be explained later, the region $\mathcal{X}$ where $U(x)$ is convex plays an important role in stability analysis using passivity that does not depend on the equilibrium point.

COFFEE BREAK

Convex function: A function $f(x)$ is called **convex** if, for any two points (x, y) in its domain and any $\theta \in [0, 1]$, the following inequality holds:

$$f\big(\theta x + (1-\theta)y\big) \leq \theta f(x) + (1-\theta) f(y), \qquad \forall\theta \in [0, 1]$$

In particular, if $f(x)$ is differentiable, a necessary and sufficient condition for $f(x)$ to be convex is that, for any two points (x, y),

$$f(x) \geq f(y) + \nabla f^\mathsf{T}(y)(x - y)$$

This inequality means that the graph of $f(x)$ is always above the tangent line to $f(x)$ at the point $x = y$.

Bregman Distance: In statistics, the quantity on the right-hand side of equation 10 for a convex function $U(x)$ is called the **Bregman distance** [**?**] between x and $x^\star$ with respect to $U(x)$. If $U(x)$ is chosen to be $|x|^2$, then the Bregman distance $W_{x^\star}(x)$ reduces to the Euclidean distance $|x - x^\star|^2$.

2.2.2 Analysis of the mechanical subsystem

As shown in Section **??**, the mechanical subsystem $\mathbb{F}$ is strongly passive. Similarly, we confirm that $\mathbb{F}$ in Equation 5 is also strongly passive regardless of the equilibrium point. First, the mechanical subsystem is represented in the form:

$$\mathbb{F} : \begin{cases} \dot{x}_{\mathbb{F}} = A_{\mathbb{F}} x_{\mathbb{F}} + B_{\mathbb{F}} u_{\mathbb{F}} + R_{\mathbb{F}} d^{\star}_{\mathbb{F}} \\ y_{\mathbb{F}} = C_{\mathbb{F}} x_{\mathbb{F}} \end{cases} \tag{12}$$

Here, the state $x_{\mathbb{F}}$ is a vector consisting of $\Delta\omega_i$, and $u_{\mathbb{F}}$ and $y_{\mathbb{F}}$ are vectors consisting of $u_{\mathbb{F}i}$ and $y\mathbb{F}i$, respectively. Also, $d\mathbb{F}^{\star}$ represents $P^{\star}_{\text{mech}}$, and the system matrices are:

$$A_{\mathbb{F}} := -M^{-1}D, \qquad B_{\mathbb{F}} := M^{-1}, \qquad R_{\mathbb{F}} := M^{-1}, \qquad C_{\mathbb{F}} := \omega_0 I$$

Note that the matrices M and D are diagonal matrices composed of M_i and D_i. For an arbitrarily selected equilibrium point $x^{\star}\mathbb{F} \in \mathcal{E}\mathbb{F}$, the storage function is chosen as:

$$W_{x^{\star}_{\mathbb{F}}}(x_{\mathbb{F}}) = \frac{\omega_0}{2}(x_{\mathbb{F}} - x^{\star}_{\mathbb{F}})^{\mathsf{T}} M (x_{\mathbb{F}} - x^{\star}_{\mathbb{F}}) \tag{13}$$

Here, $(x^{\star}\mathbb{F}, u^{\star}\mathbb{F}, y^{\star}\mathbb{F})$ with respect to the equilibrium point satisfies:

$$0 = A_{\mathbb{F}} x^{\star}_{\mathbb{F}} + B_{\mathbb{F}} u^{\star}_{\mathbb{F}} + R_{\mathbb{F}} d^{\star}_{\mathbb{F}}, \qquad y^{\star}_{\mathbb{F}} = C_{\mathbb{F}} x^{\star}_{\mathbb{F}} \tag{14}$$

If expressed in the form of Equation 10, the storage function can be written as:

$$U_{\mathbb{F}}(x_{\mathbb{F}}) := \frac{\omega_0}{2} x^{\mathsf{T}}_{\mathbb{F}} M x_{\mathbb{F}}$$

Therefore, the storage function can be expressed as:

$$W_{x^{\star}_{\mathbb{F}}}(x_{\mathbb{F}}) = U_{\mathbb{F}}(x_{\mathbb{F}}) - U_{\mathbb{F}}(x^{\star}_{\mathbb{F}}) - \nabla U^{\mathsf{T}}_{\mathbb{F}}(x^{\star}_{\mathbb{F}})(x_{\mathbb{F}} - x^{\star}_{\mathbb{F}})$$

The gradient function of this storage function can be expressed as:

$$\nabla W_{x^{\star}_{\mathbb{F}}}(x_{\mathbb{F}}) = \omega_0 M (x_{\mathbb{F}} - x^{\star}_{\mathbb{F}})$$

Hence, the time derivative of the storage function can be evaluated as:

$$\begin{aligned} \frac{d}{dt} W_{x^{\star}_{\mathbb{F}}}\left(x_{\mathbb{F}}(t)\right) &= \nabla W^{\mathsf{T}}_{x^{\star}_{\mathbb{F}}}\left(x_{\mathbb{F}}(t)\right) \dot{x}_{\mathbb{F}}(t) \\ &= \nabla W^{\mathsf{T}}_{x^{\star}_{\mathbb{F}}}\left(x_{\mathbb{F}}(t)\right) \left\{ A_{\mathbb{F}} \left(x_{\mathbb{F}}(t) - x^{\star}_{\mathbb{F}}\right) + B_{\mathbb{F}} \left(u_{\mathbb{F}}(t) - u^{\star}_{\mathbb{F}}\right) \right\} \\ &\leq (y_{\mathbb{F}}(t) - y^{\star}_{\mathbb{F}})^{\mathsf{T}} (u_{\mathbb{F}}(t) - u^{\star}_{\mathbb{F}}) - \frac{\min\{D_i\}}{\omega_0} \| y_{\mathbb{F}}(t) - y^{\star}_{\mathbb{F}} \|^2 \end{aligned} \tag{15}$$

Here, the derivation of the second equality used the relationship in Equation 14.

2.2.3 Analysis of feedback system for mechanical subsystem and automatic power generation controller

Similar to the mechanical subsystem, the passivity of the broadcast-type PI controller in equation 7 can also be demonstrated. By defining the storage function as:

$$W_{\xi^\star}(\xi) := \frac{1}{2}k_{\mathrm{I}}(\xi - \xi^\star)^2 \tag{16}$$

its time derivative can be evaluated as:

$$\begin{aligned}\frac{d}{dt}W_{\xi^\star}\left(\xi(t)\right) &= (y_{\mathbb{K}} - y_{\mathbb{K}}^\star)^{\mathsf{T}}(u_{\mathbb{K}} - u_{\mathbb{K}}^\star) - k_{\mathrm{P}}u_{\mathbb{K}}^{\mathsf{T}}hh^{\mathsf{T}}u_{\mathbb{K}} \\ &\leq (y_{\mathbb{K}} - y_{\mathbb{K}}^\star)^{\mathsf{T}}(u_{\mathbb{K}} - u_{\mathbb{K}}^\star)\end{aligned} \tag{17}$$

where $(\xi^\star, u_{\mathbb{K}}^\star, y_{\mathbb{K}}^\star)$ represents the equilibrium point and Equation 18 is used.

$$\begin{cases} 0 = h^{\mathsf{T}}u_{\mathbb{K}}^\star \\ y_{\mathbb{K}}^\star = h\left(k_{\mathrm{P}}h^{\mathsf{T}}u_{\mathbb{K}}^\star + k_{\mathrm{I}}\xi^\star\right) \end{cases} \tag{18}$$

In system control engineering, it is known that a negative feedback system between two passive systems becomes passive again. Based on this fact, a feedback connection is made between the mechanical subsystem $\mathbb{F}$ in Equation 5 and the broadcast-type PI controller $\mathbb{K}$ in Equation 7, resulting in the system:

$$\mathbb{F}_+ : \begin{cases} M\Delta\dot{\omega} = -D\Delta\omega - h\left(k_{\mathrm{P}}h^{\mathsf{T}}\Delta\omega + k_{\mathrm{I}}\xi\right) + P_{\mathrm{mech}}^\star + v_{\mathbb{F}} \\ \dot{\xi} = h^{\mathsf{T}}\Delta\omega \\ y_{\mathbb{F}} = \omega_0\Delta\omega \end{cases} \tag{19}$$

which is strongly passive regardless of the equilibrium point. In fact, adding the inequalities in Equation 15 and Equation 17, we obtain:

$$\begin{aligned}&\frac{d}{dt}\left\{W_{x_{\mathbb{F}}^\star}\left(x_{\mathbb{F}}(t)\right) + \omega_0 W_{\xi^\star}\left(\xi(t)\right)\right\} \\ &\qquad \leq (y_{\mathbb{F}}(t) - y_{\mathbb{F}}^\star)^{\mathsf{T}}(v_{\mathbb{F}}(t) - v_{\mathbb{F}}^\star) - \frac{\min\{D_i\}}{\omega_0}\|y_{\mathbb{F}}(t) - y_{\mathbb{F}}^\star\|^2\end{aligned} \tag{20}$$

where Equation 8a is used for the input-output relationship.

Furthermore, by using the input-output relationship in equation 8b, combining the machine subsystem $\mathbb{F}_+$ in equation 19 with $\mathbb{G}$ in equation 6 represents the entire feedback control system incorporating automatic generation control. Based on this fact, we analyze the passivity of $\mathbb{G}$ independent of the equilibrium point below.

2.2.4 Analysis of the electrical subsystem

We analyze the passivity of the electrical subsystem $\mathbb{G}$ in equation (6) independent of its equilibrium point. Here, we represent the column vector containing the time-varying variables δ_i, E_i, $|\boldsymbol{V}_i|$, and $\angle \boldsymbol{V}i$ related to the generator bus and load bus of $\mathbb{G}$ as $x\mathbb{G}$. Under this notation, we define the potential energy function as follows:

$$\begin{aligned} U_{\mathbb{G}}(x_{\mathbb{G}}) := &\sum_{i=1}^{n} \left\{ \frac{X_i E_i^2}{2X_i'(X_i - X_i')} - \frac{E_i|\boldsymbol{V}_i|}{X_i'} \cos(\delta_i - \angle \boldsymbol{V}_i) + \frac{|\boldsymbol{V}_i|^2}{2X_i'} \right\} \\ &- \sum_{i=n+1}^{n+m} \left\{ P^{\star}_{\text{load}i} \angle \boldsymbol{V}_i + Q^{\star}_{\text{load}i} \ln |\boldsymbol{V}_i| \right\} \\ &- \sum_{i=1}^{N} \sum_{j=1}^{N} \frac{B_{ij}}{2} |\boldsymbol{V}_i||\boldsymbol{V}_j| \cos(\angle \boldsymbol{V}_i - \angle \boldsymbol{V}_j) \end{aligned} \tag{21}$$

This potential energy function has been used, for example, in the stability analysis of power systems consisting of a single-axis generator model and a constant power load model, as described in [**?**, **?**, **?**]. Based on the expression in Equation (10), a candidate storage function is constructed as follows:

$$W_{x^{\star}_{\mathbb{G}}}(x_{\mathbb{G}}) = U_{\mathbb{G}}(x_{\mathbb{G}}) - U_{\mathbb{G}}(x^{\star}_{\mathbb{G}}) - \nabla U_{\mathbb{G}}^{\mathsf{T}}(x^{\star}_{\mathbb{G}})(x_{\mathbb{G}} - x^{\star}_{\mathbb{G}}) \tag{22}$$

Its gradient function is:

$$\nabla W_{x^{\star}_{\mathbb{G}}}(x_{\mathbb{G}}) = \nabla U_{\mathbb{G}}(x_{\mathbb{G}}) - \nabla U_{\mathbb{G}}(x^{\star}_{\mathbb{G}})$$

To calculate the time derivative of the storage function, we need to find the gradient function of the potential energy function. First, we calculate the partial derivatives of $U_{\mathbb{G}}(x_{\mathbb{G}})$ with respect to δ_i and E_i, which are given by:

$$\begin{aligned} \frac{\partial U_{\mathbb{G}}}{\partial \delta_i}(x_{\mathbb{G}}) &= \frac{E_i|\boldsymbol{V}_i|}{X_i'} \sin(\delta_i - \angle \boldsymbol{V}_i), \\ \frac{\partial U_{\mathbb{G}}}{\partial E_i}(x_{\mathbb{G}}) &= -\frac{1}{X_i - X_i'} \left\{ -\frac{X_i}{X_i'} E_i + \left(\frac{X_i}{X_i'} - 1 \right) |\boldsymbol{V}_i| \cos(\delta_i - \angle \boldsymbol{V}_i) \right\} \end{aligned}$$

Therefore, if each variable follows the differential-algebraic equation of Equation (6), because of Equation 6a, the following is true for all $i \in \mathcal{I}_{\mathbb{G}}$:

$$\frac{\partial U_{\mathbb{G}}}{\partial \delta_i}(x_{\mathbb{G}}) = y_{\mathbb{G}_i}, \qquad \frac{\partial U_{\mathbb{G}}}{\partial E_i}(x_{\mathbb{G}}) = \frac{V^{\star}_{\text{field}i} - \tau_i \dot{E}_i}{X_i - X_i'}$$

The partial derivatives of the potential energy function with respect to the voltage phase variables for $i \in \mathcal{I}_{\mathbb{G}}$ are given by:

$$\frac{\partial U_{\mathbb{G}}}{\partial |\boldsymbol{V}_i|}(x_{\mathbb{G}}) = -\sum_{j=1}^{N} B_{ij}|\boldsymbol{V}_j|\cos(\angle \boldsymbol{V}_i - \angle \boldsymbol{V}_j) - \frac{Q_i}{|\boldsymbol{V}_i|}$$
$$\frac{\partial U_{\mathbb{G}}}{\partial \angle \boldsymbol{V}_i}(x_{\mathbb{G}}) = \sum_{j=1}^{N} B_{ij}|\boldsymbol{V}_i||\boldsymbol{V}_j|\sin(\angle \boldsymbol{V}_i - \angle \boldsymbol{V}_j) - P_i$$

Therefore, from Equation 6b, it can be seen that these are equal to 0. Similarly, from Equation 6c, for $i \in \mathcal{I}_{\mathrm{L}}$, it can be seen that:

$$\frac{\partial U_{\mathbb{G}}}{\partial |\boldsymbol{V}_i|}(x_{\mathbb{G}}) = -\sum_{j=1}^{N} B_{ij}|\boldsymbol{V}_j|\cos(\angle \boldsymbol{V}_i - \angle \boldsymbol{V}_j) - \frac{Q^{\star}_{\mathrm{load}i}}{|\boldsymbol{V}_i|}$$
$$\frac{\partial U_{\mathbb{G}}}{\partial \angle \boldsymbol{V}_i}(x_{\mathbb{G}}) = \sum_{j=1}^{N} B_{ij}|\boldsymbol{V}_i||\boldsymbol{V}_j|\sin(\angle \boldsymbol{V}_i - \angle \boldsymbol{V}_j) - P^{\star}_{\mathrm{load}i}$$

Therefore, it can be seen that for all $i \in \mathcal{I}_{\mathrm{G}} \cup \mathcal{I}_{\mathrm{L}}$:

$$\frac{\partial U_{\mathbb{G}}}{\partial |\boldsymbol{V}_i|}(x_{\mathbb{G}}) = 0, \qquad \frac{\partial U_{\mathbb{G}}}{\partial \angle \boldsymbol{V}_i}(x_{\mathbb{G}}) = 0$$

Next, consider the set $(x^{\star}_{\mathbb{G}}, u^{\star}_{\mathbb{G}}, y^{\star}_{\mathbb{G}})$ related to the steady-state of $\mathbb{G}$ with respect to $\nabla U\mathbb{G}(x^{\star}\mathbb{G})$. From the equilibrium condition, there exists a set of voltage phasors $(|\boldsymbol{V}^{\star}_i|, \angle \boldsymbol{V}^{\star}_i)_{i \in \mathcal{I}_{\mathrm{G}} \cup \mathcal{I}_{\mathrm{L}}}$ such that:

$$\begin{cases} 0 = u^{\star}_{\mathbb{G}_i} \\ 0 = -\frac{X_i}{X'_i}E^{\star}_i + \left(\frac{X_i}{X'_i} - 1\right)|\boldsymbol{V}^{\star}_i|\cos(\delta^{\star}_i - \angle \boldsymbol{V}^{\star}_i) + V^{\star}_{\mathrm{field}i} \\ \begin{cases} P^{\star}_i = \sum_{j=1}^{N} B_{ij}|\boldsymbol{V}^{\star}_i||\boldsymbol{V}^{\star}_j|\sin(\angle \boldsymbol{V}^{\star}_i - \angle \boldsymbol{V}^{\star}_j) \\ Q^{\star}_i = -\sum_{j=1}^{N} B_{ij}|\boldsymbol{V}^{\star}_i||\boldsymbol{V}^{\star}_j|\cos(\angle \boldsymbol{V}^{\star}_i - \angle \boldsymbol{V}^{\star}_j) \end{cases} \end{cases} \tag{23a}$$

However, $i \in \mathcal{I}_{\mathrm{G}}$ and the steady-state values of active and reactive power are:

$$P^{\star}_i := \frac{E^{\star}_i|\boldsymbol{V}^{\star}_i|}{X'_i}\sin(\delta^{\star}_i - \angle \boldsymbol{V}^{\star}_i), \qquad Q^{\star}_i := \frac{E^{\star}_i|\boldsymbol{V}^{\star}_i|}{X'_i}\cos(\delta^{\star}_i - \angle \boldsymbol{V}^{\star}_i) - \frac{|\boldsymbol{V}^{\star}_i|^2}{X'_i}$$

In addition, $y^{\star}_{\mathbb{G}_i}$ represents $P^{\star}_i$. Therefore, the following holds for $i \in \mathcal{I}_{\mathrm{G}}$:

$$\frac{\partial U_{\mathbb{G}}}{\partial \delta_i}(x^{\star}_{\mathbb{G}}) = y^{\star}_{\mathbb{G}_i}, \qquad \frac{\partial U_{\mathbb{G}}}{\partial E_i}(x^{\star}_{\mathbb{G}}) = \frac{V^{\star}_{\mathrm{field}i}}{X_i - X'_i}$$

Similarly, since the following holds for all $i \in \mathcal{I}_{\mathrm{L}}$:

$$\begin{cases} P^{\star}_{\text{load}i} = \sum_{j=1}^{N} B_{ij} |\boldsymbol{V}_i^{\star}||\boldsymbol{V}_j^{\star}| \sin(\angle \boldsymbol{V}_i^{\star} - \angle \boldsymbol{V}_j^{\star}) \\ Q^{\star}_{\text{load}i} = -\sum_{j=1}^{N} B_{ij} |\boldsymbol{V}_i^{\star}||\boldsymbol{V}_j^{\star}| \cos(\angle \boldsymbol{V}_i^{\star} - \angle \boldsymbol{V}_j^{\star}) \end{cases} \tag{23b}$$

The partial differential related to the voltage phasor variables of the bus bars becomes:

$$\frac{\partial U_{\mathbb{G}}}{\partial |\boldsymbol{V}_i|}(x^{\star}_{\mathbb{G}}) = 0, \qquad \frac{\partial U_{\mathbb{G}}}{\partial \angle \boldsymbol{V}_i}(x^{\star}_{\mathbb{G}}) = 0$$

for all $i \in \mathcal{I}_{\mathrm{G}} \cup \mathcal{I}_{\mathrm{L}}$.

Based on the above calculation results, the time derivative along the solution trajectory of the storage function for $\mathbb{G}$ can be evaluated as follows:

$$\begin{aligned} \frac{d}{dt} W_{x^{\star}_{\mathbb{G}}}\big(x_{\mathbb{G}}(t)\big) &= \nabla W^{\mathsf{T}}_{x^{\star}_{\mathbb{G}}}\big(x_{\mathbb{G}}(t)\big) \dot{x}_{\mathbb{G}}(t) \\ &= \sum_{i=1}^{n} \left((u_{\mathbb{G}_i} - u^{\star}_{\mathbb{G}_i})(y_{\mathbb{G}_i} - y^{\star}_{\mathbb{G}_i}) - \frac{\tau_i}{X_i - X_i'} \dot{E}_i^2 \right) \\ &\leq (y_{\mathbb{G}} - y^{\star}_{\mathbb{G}})^{\mathsf{T}} (u_{\mathbb{G}} - u^{\star}_{\mathbb{G}}) \end{aligned} \tag{24}$$

where we used $u^{\star}_{\mathbb{G}} = 0$ from equation 23a. This implies that the function $W_{x^{\star}_{\mathbb{G}}}(x\mathbb{G})$ in Equation 22 is a passive storage function independent of the equilibrium point of the electrical subsystem $\mathbb{G}$. Note that the domains of $x_{\mathbb{G}}$ and $x^{\star}_{\mathbb{G}}$ are limited to the region where $W_{x^{\star}_{\mathbb{G}}}(x_{\mathbb{G}})$ is a semi-positive definite function, that is, the region where the potential energy function $U_{\mathbb{G}}(x_{\mathbb{G}})$ in Equation 21 is a convex function. This will be discussed in the next section.

2.3 Stability analysis of frequency stabilization control system

2.3.1 Stability analysis of unknown equilibrium points based on passivity

In the following, we analyze the stability of a feedback control system with automatic generation control, using passivity-based stability analysis of the linearized model as in Section **??**, but assuming that the value of the storage function given by equation 22, $W_{x^{\star}_{\mathbb{G}}}\big(x_{\mathbb{G}}(t)\big)$, is non-negative for all times t, for the trajectory $x_{\mathbb{G}}(t)$ of the electrical subsystem $\mathbb{G}$. We discuss this assumption in the next subsection.

Using the relationship of Equation 8b to the sum of inequalities in Equation 20 and Equation 24, we obtain the following for the entire feedback control system.

$$\frac{d}{dt}\left\{W_{x_{\mathbb{F}}^\star}\left(x_{\mathbb{F}}(t)\right) + \omega_0 W_{\xi^\star}\left(\xi(t)\right) + W_{x_{\mathbb{G}}^\star}\left(x_{\mathbb{G}}(t)\right)\right\} \leq -\frac{\min\{D_i\}}{\omega_0}\|y_{\mathbb{F}}(t) - y_{\mathbb{F}}^\star\|^2$$

From this inequality, it can be seen that the sum of the storage functions is monotonically non-increasing. Moreover, since the lower bound is 0, the sum asymptotically converges to a certain value as time passes. That is, the time derivative of the left-hand side asymptotically approaches 0. Therefore, it follows that:

$$\lim_{t\to\infty} y_{\mathbb{F}}(t) = y_{\mathbb{F}}^\star$$

Furthermore, focusing on the output equation of equation 5, the output $y_{\mathbb{F}}$ is a constant multiple of the internal state $\Delta\omega$, and therefore for the mechanical subsystem $\mathbb{F}$, the following holds:

$$y_{\mathbb{F}}(t) = y_{\mathbb{F}}^\star, \quad \forall t \geq 0 \qquad \Longrightarrow \qquad \Delta\omega(t) = \frac{1}{\omega_0} y_{\mathbb{F}}^\star, \quad \forall t \geq 0 \tag{25}$$

Furthermore, as analyzed in Section **??**, the frequency derivation of all generators converges on the same value. This fact implies that there exists a constant γ_0 such that:

$$y_{\mathbb{F}}^\star = \gamma_0 \mathbb{1}$$

On the other hand, from the first equation of Equation 18, we have:

$$0 = h^\mathsf{T} u_{\mathbb{K}}^\star = \frac{1}{\omega_0} h^\mathsf{T} y_{\mathbb{F}}^\star = \frac{\gamma_0}{\omega_0} h^\mathsf{T} \mathbb{1}$$

Here, since $h^\mathsf{T}\mathbb{1}$ is not zero, it is inferred that γ_0 is zero. Therefore, it is shown that the angular frequency deviation of all generators converges to zero asymptotically, that is:

$$\lim_{t\to\infty} \Delta\omega(t) = 0$$

Additionally, it is also understood that, for all $i \in \mathcal{I}_{\mathrm{G}}$, the following holds:

$$\lim_{t\to\infty} P_{\mathrm{mech}i}(t) = \lim_{t\to\infty} P_i(t)$$

However, the convergence values of the mechanical inputs and effective power are generally impossible to calculate in advance because the power consumption of loads and the impedance of transmission lines, etc., are unknown in reality. Similarly, the internal states of the electrical subsystem $\mathbb{G}$ and the voltage phase variables of the busbars in Equation 6 also converge to unknown values asymptotically.

Example 1.3 Time variation of stored energy Consider a power system model consisting of two generators and a constant power load model, as in Examples 1.1 and 1.2. The admittance value of the transmission line is set to the value in Equation **??** with the conductance component set to 0. The physical constants of the generators

Table 2 Temporal change of accumulated energy

	Bus 1	Bus 2	Bus 3
$P_i^\star$	2.5000	−3	0.5
$Q_i^\star$	0.1044	0	0.0365
$\lvert V_i^\star \rvert$	2	1.9984	2
$\angle V_i^\star$	0	−0.0539	−0.0420

(a) Steady-state power flow state 1

	Bus 1	Bus 2	Bus 3
$P_i^\star$	0.5	−3	2.5000
$Q_i^\star$	0.0432	0	0.1111
$\lvert V_i^\star \rvert$	2	1.9983	2
$\angle V_i^\star$	−0.0488	−0.0595	0

(b) Steady-state power flow state 2

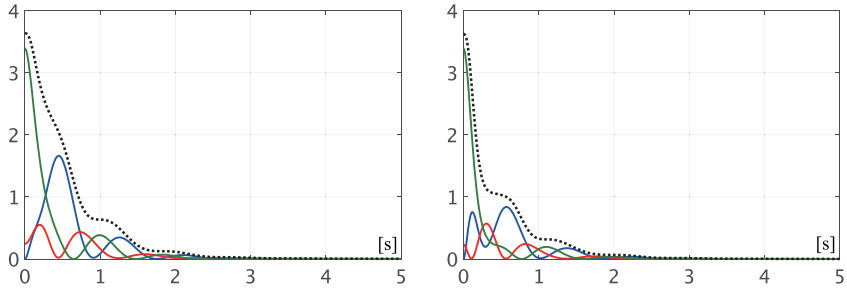

(a) Initial values corresponding to steady-state condition 1

(b) Initial values corresponding to steady-state condition 2

Fig. 5 The time variation of the storage function for the initial value response
(Blue: $W_{x_{\mathbb{F}}^\star}$, Red:$W_{x_{\mathbb{G}}^\star}$, Green: $W_{\xi^\star}$, Black: Total sum)

are set as in Examples 1.1 and 1.2. The broadcast-type PI controller in Equation 4 is set with the parameters in Table 1 (b).

For the initial values of the generators, the steady-state values corresponding to the two steady-state flow states shown in Table 2 are set. The time response of the power system until the steady-state flow state in which the active power of generators 1 and 3 are equal is achieved is then calculated. The values of $W_{x_{\mathbb{F}}^\star}(x_{\mathbb{F}})$ in Equation 13, $W_{\xi^\star}(\xi)$ in Equation 16, and $W_{x_{\mathbb{G}}^\star}(x_{\mathbb{G}})$ in Equation 22 are calculated for the time response, and the results are shown in Figure 5 (a) and (b). The blue, red, and green solid lines represent $W_{x_{\mathbb{F}}^\star}(x_{\mathbb{F}})$, $W_{x_{\mathbb{G}}^\star}(x_{\mathbb{G}})$, and $W_{\xi^\star}(\xi)$, respectively. The black dashed line represents their sum. From these figures, it can be seen that while exchanging energy among the three components, the total energy of the entire power system monotonically decreases.

2.3.2 The range where the potential energy function is convex

In the following, we show that the conditions for the potential energy function $U_{\mathbb{G}}(x_{\mathbb{G}})$ in Equation 21 to be a convex function correspond to the passive power

transmission conditions (i) and (iii) discussed in Definition **??** in the analysis of the passive properties of the linear approximation model. Note that assumption (ii) of the passive power transmission conditions is assumed in this section.

We consider the case where generators are connected to all buses, in accordance with the setting of the linear approximation model in Section **??**. That is, the subscripts for the generator buses and load buses are

$$\mathcal{I}_{\mathrm{G}} = \{1, \ldots, N\}, \qquad \mathcal{I}_{\mathrm{L}} = \emptyset$$

In this case, applying the Kron reduction to the generator buses allows us to obtain an equivalent system of ordinary differential equations for the electrical subsystem $\mathbb{G}$ in Equation 6, with respect to $i \in \mathcal{I}_{\mathrm{G}}$, given by:

$$\mathbb{G}_i : \begin{cases} \dot{\delta}_i = u_{\mathbb{G}_i} \\ \tau_i \dot{E}_i = -\frac{X_i}{X_i'} E_i - \left(X_i - X_i'\right) \sum_{j=1}^{N} E_j B_{ij}^{\mathrm{red}} \cos \delta_{ij} + V_{\mathrm{field}i}^{\star} \\ y_{\mathbb{G}_i} = -E_i \sum_{j=1}^{N} E_j B_{ij}^{\mathrm{red}} \sin \delta_{ij} \end{cases}$$

where δ_{ij} denotes $\delta_i - \delta_j$. Also, the reduced susceptance B_{ij}^{red} is defined as the (i, j)-th element of the matrix B^{red}, which is obtained by combining the susceptance matrix B of the power network in Eq. (6), and is defined as follows:

$$B^{\mathrm{red}} := -\left\{\mathrm{diag}\left(X_i'\right) - \mathrm{diag}\left(X_i'\right) B \, \mathrm{diag}\left(X_i'\right)\right\}^{-1} \tag{26}$$

The potential energy function corresponding to the representation of this system of ordinary differential equations is given by Equation 21. It is expressed as follows in Equation 27:

$$U_{\mathbb{G}}^{\mathrm{red}}(z_{\mathbb{G}}) := \frac{1}{2} \sum_{i=1}^{N} \left\{ \frac{X_i E_i^2}{X_i'(X_i - X_i')} + E_i \sum_{j=1}^{N} E_j B_{ij}^{\mathrm{red}} \cos \delta_{ij} \right\} \tag{27}$$

where the vector with all δ_i and E_i is expressed as $z_{\mathbb{G}}$. If we calculate the partial differential related to the internal state, the following is obtained:

$$\frac{\partial U_{\mathbb{G}}^{\mathrm{red}}}{\partial \delta_i}(z_{\mathbb{G}}) = y_{\mathbb{G}_i}, \qquad \frac{\partial U_{\mathbb{G}}^{\mathrm{red}}}{\partial E_i}(z_{\mathbb{G}}) = \frac{V_{\mathrm{field}i}^{\star} - \tau_i \dot{E}_i}{X_i - X_i'}$$

Similarly, for the steady state, we have:

$$\frac{\partial U_{\mathbb{G}}^{\mathrm{red}}}{\partial \delta_i}(z_{\mathbb{G}}^{\star}) = y_{\mathbb{G}_i}^{\star}, \qquad \frac{\partial U_{\mathbb{G}}^{\mathrm{red}}}{\partial E_i}(z_{\mathbb{G}}^{\star}) = \frac{V_{\mathrm{field}i}^{\star}}{X_i - X_i'}$$

Therefore, if we define the corresponding storage function as:

$$W^{\text{red}}_{z^\star_{\mathbb{G}}}(z_{\mathbb{G}}) = U^{\text{red}}_{\mathbb{G}}(z_{\mathbb{G}}) - U^{\text{red}}_{\mathbb{G}}(z^\star_{\mathbb{G}}) - \left\{\nabla U^{\text{red}}_{\mathbb{G}}(z^\star_{\mathbb{G}})\right\}^{\mathsf{T}} (z_{\mathbb{G}} - z^\star_{\mathbb{G}})$$

Then, similarly to Equation 24, its time derivative can be bounded as:

$$\frac{d}{dt} W^{\text{red}}_{z^\star_{\mathbb{G}}}\big(z_{\mathbb{G}}(t)\big) \leq (y_{\mathbb{G}} - y^\star_{\mathbb{G}})^{\mathsf{T}} (u_{\mathbb{G}} - u^\star_{\mathbb{G}})$$

Note that all elements of the reduced susceptance matrix B^{red} in Equation 26 are non-positive. This fact can be shown as follows. From the discussion in the Section **??**, the susceptance matrix B is a negative definite matrix with non-diagonal elements that are nonnegative. Therefore:

$$B_{-} := \mathsf{diag}\left(X'_i\right) - \mathsf{diag}\left(X'_i\right) B\, \mathsf{diag}\left(X'_i\right)$$

is a positive definite matrix with non-positive off-diagonal elements, known as an **M-matrix**. It is known that all elements of the inverse of an M-matrix are non-negative [**?**]. Therefore, all elements of $B^{\text{red}} = -B_{-}^{-1}$ are non-positive.

COFFEE BREAK

Hessian matrix: A condition necessary for a twice-differentiable function $f : \mathbb{R}^n \to \mathbb{R}$ to be a convex over a certain range $\mathcal{X}$ is that the following matrix is positive semi-definite for all $x \in \mathcal{X}$:

$$\nabla^2 f(x) := \begin{bmatrix} \frac{\partial^2 f}{\partial x_1^2}(x) & \cdots & \frac{\partial^2 f}{\partial x_1 \partial x_n}(x) \\ \vdots & \ddots & \vdots \\ \frac{\partial^2 f}{\partial x_n \partial x_1}(x) & \cdots & \frac{\partial^2 f}{\partial x_n^2}(x) \end{bmatrix}$$

This matrix is called the **Hessian matrix** of the function f [**?**].

The convexity of the potential energy function $U^{\text{red}}_{\mathbb{G}}(z_{\mathbb{G}})$ in Equation 27 is characterized by the positive semidefiniteness of its Hessian matrix $\nabla^2 U^{\text{red}}_{\mathbb{G}}(z_{\mathbb{G}})$. Computing this Hessian matrix yields to:

$$\nabla^2 U^{\text{red}}_{\mathbb{G}}(z_{\mathbb{G}}) = \begin{bmatrix} L(z_{\mathbb{G}}) & -\hat{B}^{\mathsf{T}}(z_{\mathbb{G}}) \\ -\hat{B}(z_{\mathbb{G}}) & -\hat{A}(z_{\mathbb{G}}) \end{bmatrix} \tag{28}$$

However, the matrix constituting each block has the element (i, j) given by:

$$L_{ij}(z_{\mathbb{G}}) := \frac{\partial^2 U^{\text{red}}_{\mathbb{G}}}{\partial \delta_i \partial \delta_j}(z_{\mathbb{G}}) = \begin{cases} -E_i \sum_{j=1, j\neq i}^{N} E_j B^{\text{red}}_{ij} \cos(\delta_{ij}), & i = j \\ E_i E_j B^{\text{red}}_{ij} \cos(\delta_{ij}), & i \neq j \end{cases}$$

$$\hat{A}_{ij}(z_{\mathbb{G}}) := -\frac{\partial^2 U^{\text{red}}_{\mathbb{G}}}{\partial E_i \partial E_j}(z_{\mathbb{G}}) = \begin{cases} -\left(B^{\text{red}}_{ii} + \frac{X_i}{X'_i(X_i - X'_i)}\right), & i = j \\ -B^{\text{red}}_{ij} \cos(\delta_{ij}), & i \neq j \end{cases}$$

$$\hat{B}_{ij}(z_{\mathbb{G}}) := -\frac{\partial^2 U^{\text{red}}_{\mathbb{G}}}{\partial E_i \partial \delta_j}(z_{\mathbb{G}}) = \begin{cases} \sum_{j=1, j\neq i}^{N} E_j B^{\text{red}}_{ij} \sin(\delta_{ij}), & i = j \\ -E_j B^{\text{red}}_{ij} \sin(\delta_{ij}), & i \neq j \end{cases}$$

The Hessian matrix evaluated at the equilibrium point in Equation 28, $\nabla^2 U_{\mathbb{G}}^{\mathrm{red}}(z_{\mathbb{G}}^{\star})$, is identical to the matrix P_G in Equation **??**, which appeared in the passive analysis of the linearized electric subsystem in Section **??**. Note that the positive semi-definiteness of P_G guarantees that the accumulation function for demonstrating the passivity of the linearized model of $\mathbb{G}$ is a positive semi-definite function. Therefore, it is understood that the necessary and sufficient condition for $U_{\mathbb{G}}^{\mathrm{red}}(z_{\mathbb{G}}^{\star})$ to be a convex function is equivalent to the necessary and sufficient condition for P_G to be positive semi-definite, which is equivalent to the passive power transmission conditions (i) and (iii) being satisfied.

In combination with the results from Section **??**, it can be understood that the region defined as the convex set of the potential energy function $U_{\mathbb{G}}^{\mathrm{red}}(z_{\mathbb{G}})$ given in Equation 27:

$$\mathcal{E}_{\mathbb{G}} := \left\{ z_{\mathbb{G}}^{\star} : \nabla^2 U_{\mathbb{G}}^{\mathrm{red}}(z_{\mathbb{G}}^{\star}) \geq 0 \right\}$$

is also the "maximum" set of equilibrium points that can demonstrate frequency stability based on passivity.

The reason for this is that the passive power transmission conditions are necessary conditions for the linearized electric subsystem to be passive in the vicinity of a specific equilibrium point, as shown in Section **??**. Therefore, for equilibrium points $z_{\mathbb{G}}^{\star}$ where $\nabla^2 U_{\mathbb{G}}^{\mathrm{red}}(z_{\mathbb{G}}^{\star})$ is not positive semi-definite, the electric subsystem $\mathbb{G}$ cannot be passive.

On the other hand, if the initial value of the electrical subsystem $z_{\mathbb{G}}(0)$ is set in the vicinity of a certain equilibrium point $z_{\mathbb{G}}^{\star}$ belonging to the set $\mathcal{E}_{\mathbb{G}}$, then for all combinations of physical parameters $(M_i, D_i, \tau_i)_{i \in \mathcal{I}_{\mathbb{G}}}$, the entire feedback control system will asymptotically converge to a steady-state power flow state where demand and supply are balanced.

For example, consider a situation where the power consumption of a certain load changes in a stepwise and small manner from a steady-state power flow state where demand and supply are balanced. In this case, since the equilibrium point of the electrical subsystem $\mathbb{G}$ undergoes a small variation from the original steady-state power flow state to the new one, the initial time can be regarded as the time when the power consumption changes and the initial value of $\mathbb{G}$ can be set in the vicinity of the equilibrium point.

From the above analytical result, it can be concluded that as long as the time variation of model parameters such as loads and controller parameters is sufficiently gradual and the power system state remains in the region where the potential energy function becomes a convex function, frequency stability is maintained by automatic generation control.

3 Transient stability control

3.1 Decentralized control of generators with excitation system

In power system engineering, the term **transient stability** is widely used when discussing the size and stability of the stability region of the equilibrium point. In this section, we outline the mathematical models and characteristics of **excitation systems** implemented for the purpose of increasing the transient stability of the power system. Excitation systems are generally local controllers implemented "individually" for each generator, which perform control operations that automatically adjust the field input by locally measuring the voltage phase or current phase of the bus to which the generator is connected, as well as the internal state of the generator. The main element of an excitation system is the **Automatic Voltage Regulator** (AVR), a control device that maintains the bus voltage at the desired value. In addition, to suppress oscillations caused by the AVR, additional control algorithms called **Power System Stabilizers** (PSS) may also be incorporated. In Sections 3.2 to 3.5, we will explain these standard models and control effects.

3.2 Standard Automatic Voltage Regulator model

There are many standardized models for automatic voltage regulators. For example, the IEEE's standardization report [**?**] lists more than 40 standard models. Automatic voltage regulator models are broadly classified into direct current (DC), alternating current (AC), and static types. In the following, we describe representative models of DC and static types.

First, we describe the **IEEE Type DC1 excitation system model**, which is a direct current (DC) model of the automatic voltage regulator. For detailed modeling, please refer to [**?**, Section 7.9.2] or [**?**, Section 8.6.3]. Here, we discuss the automatic voltage regulator for a generator connected to bus i. To simplify the notation, we omit the subscript i. Specifically, we use the generator model discussed in Section **??**:

$$\begin{cases} \dot{\delta} = \omega_0 \Delta\omega \\ M\Delta\dot{\omega} = -D\Delta\omega - P + P_{\text{mech}} \\ \tau\dot{E} = -I_{\text{field}} + V_{\text{field}} \end{cases} \tag{29}$$

However, for the sake of the following discussion, we define the value of the excitation current of the generator in the units of pu as:

$$I_{\text{field}} := \frac{X}{X'}E - \left(\frac{X}{X'} - 1\right)|\boldsymbol{V}|\cos(\delta - \angle \boldsymbol{V}) \tag{30}$$

The active and reactive powers output by the generator are given by:

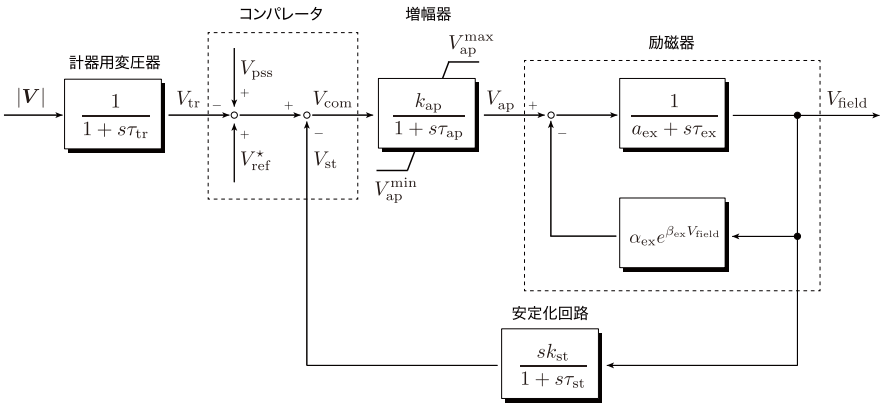

Fig. 6 IEEE DC1 type model of automatic voltage regulator

$$P = \frac{E|\boldsymbol{V}|}{X'}\sin(\delta - \angle\boldsymbol{V}), \qquad Q = \frac{E|\boldsymbol{V}|}{X'}\cos(\delta - \angle\boldsymbol{V}) - \frac{|\boldsymbol{V}|^2}{X'}$$

It should be noted that for the salient-pole generator model discussed in section **??**, we replace X' and X in Equation 30 with $X'_{\rm d}$ and $X_{\rm d}$, respectively, to define $I_{\rm field}$.

As shown in Figure 6, the IEEE DC1 model of the automatic voltage regulator is a controller that takes the magnitude $|\boldsymbol{V}|$ of the bus voltage phasor as input and outputs the field excitation input $V_{\rm field}$ of the generator. However, as additional input signals, a reference signal $V_{\rm ref}^{\star}$ for adjusting the magnitude of the bus voltage phasor to the desired value and a control signal $V_{\rm pss}$ output by the power system stabilizer are applied. The IEEE DC1 model of the automatic voltage regulator consists of four basic devices: a voltage transformer, a comparator, an amplifier, and an exciter, as well as an auxiliary stabilizing circuit. In the following, we will explain the dynamic characteristics of each device.

3.2.1 Voltage transformer

The voltage transformer is a device that reduces the bus voltage to a voltage that can be used by the control circuit, and its dynamic characteristics is modeled as a first-order lag filter:

$$\tau_{\rm tr}\dot{V}_{\rm tr} = -V_{\rm tr} + |\boldsymbol{V}| \tag{31a}$$

Generally, the time constant $\tau_{\rm tr}$ is sufficiently small, and the output $V_{\rm tr}$ of the voltage transformer is almost equal to the absolute value of the bus voltage $|\boldsymbol{V}|$.

3.2.2 Comparator

The comparator is a device that outputs the difference between the output V_{tr} of the voltage transformer and the reference signal $V_{\mathrm{ref}}^{\star}$. The output V_{pss} of the power system stabilizer mentioned later is applied as a signal to adjust the constant $V_{\mathrm{ref}}^{\star}$. In addition, when incorporating a stabilizing circuit for the excitation system, its output V_{st} is also fed back. That is, the comparator is modeled as

$$V_{\mathrm{com}} = V_{\mathrm{ref}}^{\star} + V_{\mathrm{pss}} - V_{\mathrm{tr}} - V_{\mathrm{st}} \tag{31b}$$

As mentioned above, since V_{tr} is almost equal to $|\boldsymbol{V}|$ because the time constant τ_{tr} is usually very small, if the output V_{pss} of the power system stabilizer and the output V_{st} of the stabilizing circuit are zero, the output V_{com} of the comparator is almost equal to the difference between the reference signal and the absolute value of the bus voltage phase $V_{\mathrm{ref}}^{\star} - |\boldsymbol{V}|$.

3.2.3 Amplifier

The amplifier is a device that amplifies the output V_{com} of the comparator to drive the excitation system. There are various types, such as rotary and electromagnetic types, but in many cases, it is modeled as:

$$\tau_{\mathrm{ap}}\dot{V}_{\mathrm{ap}} = \begin{cases} -V_{\mathrm{ap}} + k_{\mathrm{ap}}V_{\mathrm{com}}, & V_{\mathrm{ap}}^{\mathrm{min}} < V_{\mathrm{ap}} < V_{\mathrm{ap}}^{\mathrm{max}} \ \text{ or } \ V_{\mathrm{ap}}V_{\mathrm{com}} \leq 0 \\ 0, & \text{otherwise} \end{cases} \tag{31c}$$

where the time constant τ_{ap} and gain k_{ap} are non-negative constants, and the saturation that constrains the internal state V_{ap} to the range $[V_{\mathrm{ap}}^{\mathrm{min}}, V_{\mathrm{ap}}^{\mathrm{max}}]$ is expressed by the conditional branching. Note that in some cases, saturation is applied to the output instead of the internal state, and in transient states with large disturbances such as ground faults, the width of the saturation limits may be set large [**?**, Section 4.3].

3.2.4 Exciter

The exciter is a device that generates the field input V_{field} from the output $V_{\mathrm{ap}}^{\mathrm{sat}}$ of the amplifier, modeled as a nonlinear first-order system given by:

$$\tau_{\mathrm{ex}}\dot{V}_{\mathrm{field}} = -\Big(a_{\mathrm{ex}} + \underbrace{\alpha_{\mathrm{ex}}e^{\beta_{\mathrm{ex}}V_{\mathrm{field}}}}_{*}\Big)V_{\mathrm{field}} + V_{\mathrm{ap}} \tag{31d}$$

Here, τ_{ex} is a positive constant, but the sign of a_{ex} may vary depending on the literature. The term denoted by "$*$" represents the nonlinearity due to magnetic saturation and other effects within the exciter, and α_{ex} and β_{ex} are both non-negative

constants. These constants are typically set to ensure stable dynamic behavior of the exciter in the vicinity of the normal operating point.

3.2.5 Stabilizing circuit

The stabilizing circuit is a circuit that is implemented to enhance the stability of the excitation system. In the IEEE DC1 model, it is represented as a mechanism that feeds back the differential value of the field input. That is, its dynamic characteristics are expressed as:

$$\tau_{\mathrm{st}}\dot{V}_{\mathrm{st}} = -V_{\mathrm{st}} + k_{\mathrm{st}}\dot{V}_{\mathrm{field}} \tag{31e}$$

where the time constant τ_{st} and gain k_{st} are non-negative constants. The output V_{st} of this stabilization circuit is fed back to the comparator in Equation 31b.

The IEEE Type DC1 excitation system model of AVR is a combination of Equation 31a to Equation 31e discussed above. The reference values of each parameter are summarized in 3 and 4. The unit of the time constant is [s] while other units are [pu].

Table 3 Parameter example of IEEE DC1 type model

	τ_{tr}	τ_{ap}	k_{ap}	$V_{\mathrm{ap}}^{\mathrm{max}}$	$V_{\mathrm{ap}}^{\mathrm{min}}$
Example 1 [**?**, Table D.3. Unit F2]	0.00	0.05	57.1	1.00	−1.00
Exapmle 2 [**?**, Table 7.3]	0.00	0.2	20	∞	$-\infty$

Table 4 Parameter example of IEEE DC1 type model (continued)

	τ_{ex}	a_{ex}	α_{ex}	β_{ex}	τ_{st}	k_{st}
Example 1 [**?**, Table D.3. Unit F2]	0.50	−0.045	0.0012	1.21	1.00	0.08
Example 2 [**?**, Table 7.3]	0.314	1.0	0.0039	1.555	0.35	0.063

Next, we will explain the **IEEE Type ST1 excitation system model** which has a similar structure to the IEEE DC1 type but is a static model with faster response. In this automatic voltage regulator model, the excitation system time constant is sufficiently small, and the excitation system model in Equation 31d is expressed as a static relationship:

$$V_{\mathrm{field}} = \mathsf{sat}\big(V_{\mathrm{ap}}; V_{\mathrm{field}}^{\mathrm{min}}, V_{\mathrm{field}}^{\mathrm{max}}\big)$$

where sat is the output saturation function defined by:

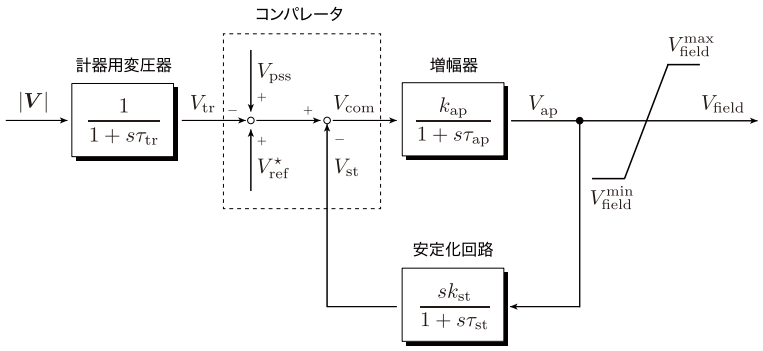

Fig. 7 IEEE ST1 type model of automatic voltage regulator

$$\mathsf{sat}(x;\underline{\alpha},\overline{\alpha}) := \begin{cases} \underline{\alpha},\ x \le \underline{\alpha} \\ x,\ \underline{\alpha} < x \le \overline{\alpha} \\ \overline{\alpha},\ x > \overline{\alpha} \end{cases}$$

Additionally, the upper and lower limits of output saturation are modeled to mainly depend on the absolute value of the bus voltage phase angle [**?**, Section 8.63]. Specifically, using $|\boldsymbol{V}|$ and $I_{\rm field}$ in Equation 29, they are given by

$$V_{\rm field}^{\rm min} = \gamma_{-}|\boldsymbol{V}|, \qquad V_{\rm field}^{\rm max} = \gamma_{+}|\boldsymbol{V}| - k_0 I_{\rm field}$$

where γ_{-}, γ_{+}, and k_0 are non-negative constants. The block diagram of this model is shown in Figure 7. Note that during a ground fault on the bus, $|\boldsymbol{V}|$ becomes 0, and the excitation input $V_{\rm field}$ is not outputted from the AVR.

Since the excitation response of the IEEE ST1 model is fast enough, stabilizing circuits are often unnecessary. When the amplifier time constant $\tau_{\rm ap}$ is small enough that its dynamic characteristics can be ignored, a simplified first-order model given by Equation 32 is used. For example, this model is used in [**?**, Section 12.4] and [**?**, Section 4.2.2]. Examples of parameters are shown in Examples 1 and 2 of Table 5.

$$\begin{cases} \tau_{\rm tr}\dot{V}_{\rm tr} = -V_{\rm tr} + |\boldsymbol{V}| \\ V_{\rm ap} = k_{\rm ap}(V_{\rm ref}^{\star} + V_{\rm pss} - V_{\rm tr}) \\ V_{\rm field} = \mathsf{sat}\left(V_{\rm ap}; V_{\rm field}^{\rm min}, V_{\rm field}^{\rm max}\right) \end{cases} \tag{32}$$

Table 5 IEEE ST1 type model parameter example

	$\tau_{\rm tr}$	$\tau_{\rm ap}$	$k_{\rm ap}$	γ_{+}	γ_{-}	k_0	$\tau_{\rm st}$	$k_{\rm st}$
Example 1 [**?**, Section 8.6.3]	0.015	0	200	7.00	−6.40	0.04	0	0
Example 2 [**?**, Table H.23]	0.02	0	210	6.43	−6.00	0.038	0	0
Example 3 [**?**, Section V]	0	0.076	36.66	∞	$-\infty$	0	0	0
Example 4 [**?**, Table 4]	0	0.05	20	∞	$-\infty$	0	0	0

When the time constant of the amplifier τ_{ap} is not zero, but the time constant of the instrument transformer τ_{tr} is zero or a model that excludes output saturation is often used [**?**, **?**, **?**], the following equation can be used:

$$\begin{cases} \tau_{\mathrm{ap}} \dot{V}_{\mathrm{ap}} = -V_{\mathrm{ap}} + k_{\mathrm{ap}} (V_{\mathrm{ref}}^{\star} + V_{\mathrm{pss}} - |\boldsymbol{V}|) \\ V_{\mathrm{field}} = V_{\mathrm{ap}} \end{cases} \tag{33}$$

Parameter examples of this model are shown in Example 3 and Example 4 of Table 5.

Note that when the desired steady-state value of the excitation input $V_{\mathrm{field}}^{\star}$ and the absolute value of the bus voltage $\left|\boldsymbol{V}^{\star}\right|$ are given, the reference signal $V_{\mathrm{ref}}^{\star}$ for the reference is determined as follows:

$$V_{\mathrm{ref}}^{\star} = \frac{V_{\mathrm{field}}^{\star}}{k_{\mathrm{ap}}} + |\boldsymbol{V}^{\star}| \tag{34}$$

However, in actual power system operation, the steady-state values of bus voltage and excitation input are unknown and can vary due to load distribution, and other factors, so the value of the reference signal $V_{\mathrm{ref}}^{\star}$ is specified using standard values for bus voltage and excitation input.

3.3 Control effectiveness of AVR

Let's analyze the control effectiveness of the Automatic Voltage Regulator (AVR) using a simple power system model.

Example 1.4 Effect of automatic voltage regulator on steady-state and transient stability

Consider the three-bus power system model discussed in Examples **??**, **??**, and **??**. The physical constants of the generator and transmission lines are set to the same values as in Example **??**. Furthermore, the load connected to bus 2 is modeled as a constant impedance, and the impedance value is set to the first row of Table **??**. The automatic voltage regulator is set to the IEEE ST1 type model in Equation 32. The automatic voltage regulator incorporated in generators 1 and 3 is identical, and the parameter values are those of Example 1 in Table 5.

First, let us examine the change in the set of steady-state stable equilibrium points due to the presence or absence of the automatic voltage regulator. Specifically, the steady-state stability of the corresponding power system is determined based on the approximate linearization by varying the difference in steady-state values of the rotor angle, $\delta_3^{\star} - \delta_1^{\star}$, while fixing the steady-state values of the internal voltage of the generators, $E_1^{\star}$ and $E_3^{\star}$, to the values in the rightmost column of Table **??**. By calculating the range of $\delta_3^{\star} - \delta_1^{\star}$ where the approximate linear model is stable, it is found that without the automatic voltage regulator, the range is as shown in (i) of Table 6, while with the automatic voltage regulator, the range is as shown in (ii) of Table 6.

From this result, it is understood that the set of stable equilibrium points tends to decrease due to the automatic voltage regulator.

Note that without loss of generality, $\delta_1^\star$ or $\delta_3^\star$ can be set to zero. In addition, if the steady-state values of the internal states of each generator are determined, the corresponding steady-state values of the mechanical and field inputs can be determined by

$$\begin{cases} P^\star_{\text{mech}i} = f_i\left(\delta^\star, E^\star\right) \\ V^\star_{\text{field}i} = \frac{X_i}{X_i'} E_i^\star - \left(X_i - X_i'\right) g_i\left(\delta^\star, E^\star\right) \end{cases} \qquad i \in \{1, 3\}$$

where $\delta^\star$ and $E^\star$ are vectors with $\delta_i^\star$ and $E_i^\star$, and functions f_i and g_i are defined by Equation **??**.

Furthermore, the steady-state value of the voltage phase of the generator bus can be obtained using Equation **??** as follows:

$$\begin{bmatrix} \boldsymbol{V}_1^\star \\ \boldsymbol{V}_3^\star \end{bmatrix} = \left(\begin{bmatrix} \frac{1}{\boldsymbol{j}X_1'} & 0 \\ 0 & \frac{1}{\boldsymbol{j}X_3'} \end{bmatrix} + \boldsymbol{Y}_{\text{Kron}} \right)^{-1} \begin{bmatrix} \frac{e^{\boldsymbol{j}\delta_1^\star}}{\boldsymbol{j}X_1'} & 0 \\ 0 & \frac{e^{\boldsymbol{j}\delta_3^\star}}{\boldsymbol{j}X_3'} \end{bmatrix} \begin{bmatrix} E_1^\star \\ E_3^\star \end{bmatrix}$$

Here, $\boldsymbol{Y}$Kron is the admittance matrix obtained by Kron reduction of the load bus defined in equation **??**. The value of the reference signal $V^\star_{\text{ref}i}$ is determined by equation 34.

Table 6 Steady value of rotor declination that stabilizes the state
(AVR: automatic voltage regulator, PSS: system stabilizer)

	(i) Without AVR	(ii) With AVR	(iii) With AVR and PSS
$\delta_3^\star - \delta_1^\star$ Upper limit [rad]	1.03	0.87	1.32
$\delta_3^\star - \delta_1^\star$ Lower limit [rad]	−0.90	−0.30	−1.10

COFFEE BREAK

$\mathcal{L}_2$ **norm**: The $\mathcal{L}_2$ **norm** of a function $y : [0, \infty) \to \mathbb{R}^n$ is defined as

$$\|y\|_{\mathcal{L}_2} := \sqrt{\int_0^\infty \|y(\tau)\|^2 d\tau}$$

This value can be interpreted as the energy of a time-varying signal. Unless the signal's amplitude decays over time, the $\mathcal{L}_2$ norm will generally be infinite. The letter "$\mathcal{L}$" comes from the name of Henri Lebesgue, who is known for his work on the theory of Lebesgue integration.

Next, let us confirm the improvement of transient stability by the automatic voltage regulator. Specifically, we will conduct the following analysis. First, regardless of the presence of the automatic voltage regulator, we consider a steady-state stability with a steady-state value of the rotor angle difference $\delta_3^\star - \delta_1^\star$ equal to $-\frac{\pi}{6}$ [rad]. The

steady-state value of the internal voltage is set to the above value. Next, we change the initial values of the power system model as parameters and calculate $\|\Delta\omega\|_{\mathcal{L}_2}$ for the time response of the obtained angular frequency deviation. Here, $\Delta\omega$ is a vector consisting of $\Delta\omega_1$ and $\Delta\omega_3$. Similarly, we calculate $||\boldsymbol{V}| - |\boldsymbol{V}^\star||\mathcal{L}_2$ for the time response of the main bus voltage phase deviation. Here, $|\boldsymbol{V}|$ is a vector consisting of $\||\boldsymbol{V}|-|\boldsymbol{V}^\star|\|_{\mathcal{L}_2}$ is a vector consisting of $|\boldsymbol{V}_1^\star|$ and $|\boldsymbol{V}_3^\star|$. Note that when the initial value is given inside the stable region of the equilibrium point of interest, the $\mathcal{L}_2$ norm values of the angular frequency deviation and the main bus voltage phase deviation are finite. Moreover, it is known that the higher the $\mathcal{L}_2$ norm values of these quantities, the higher the transient stability of the equilibrium point for the given initial values. On the other hand, when the initial value is given outside the stable region, the $\mathcal{L}_2$ norm values become infinite.

The analysis results of the transient stability are shown in Figure 8. The horizontal axis represents the initial value of $\delta_3 - \delta_1$ set, and the vertical axis represents the $\mathcal{L}_2$ norm value of the angular frequency deviation and the main bus voltage phase deviation generated for the set initial value. The case without the automatic voltage regulator corresponding to (i) in Table 6 is represented by a solid blue line, and the case with the automatic voltage regulator corresponding to (ii) is represented by a dashed black line. Note that the plots are shown for the range of initial values for which the $\mathcal{L}_2$ norm values are finite. The initial values of the internal voltage E_1 and E_3 are set to the same value as their steady-state value $E_1^\star$ and $E_3^\star$, respectively. The initial values of the angular frequency deviation $\Delta\omega_1$ and $\Delta\omega_3$ are both set to 0. From this result, it can be seen that the transient stability of the angular frequency deviation and the main bus voltage phase deviation has improved by incorporating the automatic voltage regulator. It can also be seen that the

As a reference, the time response of the angular frequency deviation that occurs when the initial value of $\delta_3 - \delta_1$ is set to -1 and $-\frac{\pi}{2}$, respectively, is shown in Figures 9 and 10. (a) represents the case without automatic voltage regulator and (b) represents the case with automatic voltage regulator. From these results, it can be seen that incorporating an automatic voltage regulator tends to make the low-frequency component (the center value) of the oscillation of the angular frequency deviation converge to 0 more quickly. On the other hand, it is also found that there is no significant change in the decay rate of the high-frequency component of the oscillation, regardless of the presence or absence of the automatic voltage regulator.

From Example 1.4, it can be seen that incorporating an automatic voltage regulator tends to destabilize some of the equilibrium points that were stable before implementation, while suppressing the low-frequency components of the oscillation of the angular frequency deviation. This means that the transient stability of the power system has improved. The system stabilization device described in the next section has the effect of suppressing the high-frequency components of the oscillation that could not be suppressed by the automatic voltage regulator.

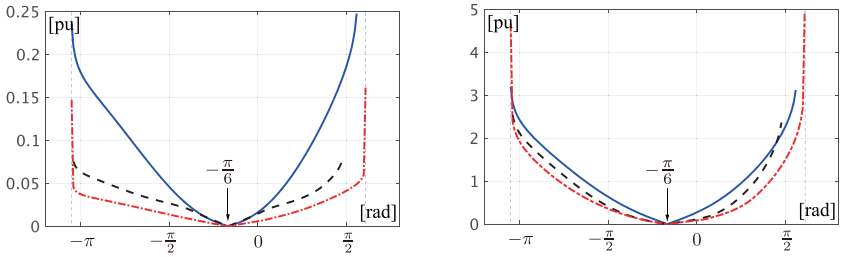

(a) $\|\Delta\omega\|_{\mathcal{L}_2}$ (b) $\left\||\boldsymbol{V}| - |\boldsymbol{V}^\star|\right\|_{\mathcal{L}_2}$

Fig. 8 Transient stability evaluation for the initial value of the rotor declination difference
(Blue solid line: (i), Black dashed line: (ii), Red chain line: (iii))

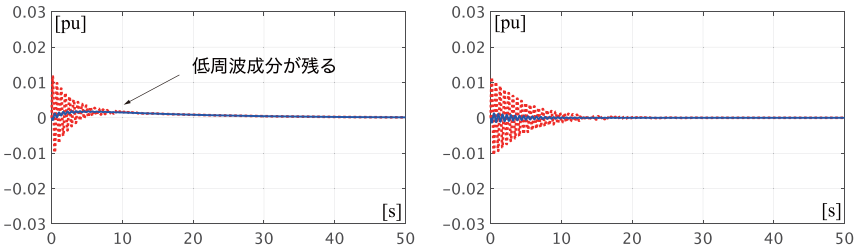

(a) Without AVR (b) With AVR

Fig. 9 Initial value response of angular frequency deviation
(Blue solid line: $\Delta\omega_1$, red dashed line: $\Delta\omega_3$)

3.4 Power System Stabilizer

A power system stabilizer (PSS) is a device that outputs an additional control signal V_{pss} as shown in Figures 6 and 7. Generally, measurements such as generator's angular frequency deviation, active power, and bus voltage phase are fed back to the PSS. Here we explain the model of a standard PSS called the **IEEE Type PSS1 power system stabilizer model** [**?**, Section 9.2]. This model mainly consists of two parts: a **washout filter** and a **phase-lead compensator**. The block diagram is shown in Figure 11.

3.4.1 Washout filter

The washout filter is a high-pass filter used in the power system stabilizer to maintain a steady-state gain of 0. It takes the generator's angular frequency deviation $\Delta\omega$,

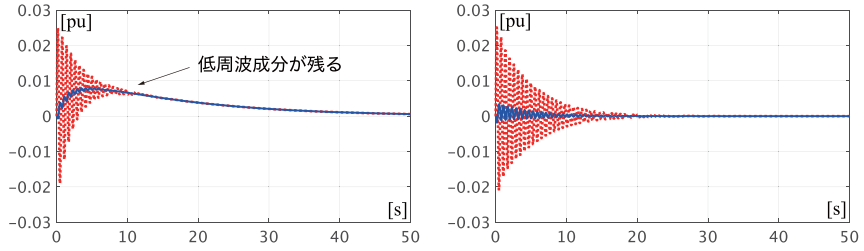

(a) Without AVR (b) With AVR

Fig. 10 Initial value response of angular frequency deviation
(Blue solid line: $\Delta\omega_1$, Red dashed line: $\Delta\omega_3$)

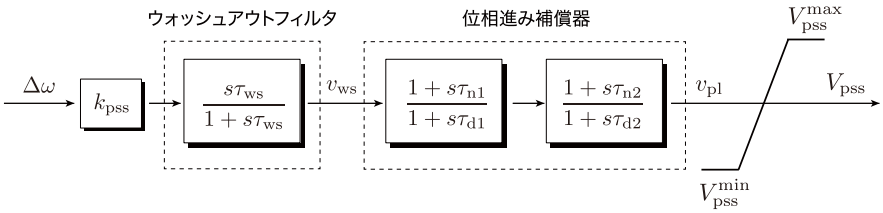

Fig. 11 IEEE PSS1 type model of system stabilizer

which is multiplied by a constant gain k_{pss}, as input, and its dynamic characteristics are expressed by the following differential equation:

$$\begin{cases} \tau_{\mathrm{ws}}\dot{\xi}_{\mathrm{ws}} = -\xi_{\mathrm{ws}} + k_{\mathrm{pss}}\Delta\omega \\ v_{\mathrm{ws}} = k_{\mathrm{pss}}\Delta\omega - \xi_{\mathrm{ws}} \end{cases} \tag{35a}$$

The steady-state output $v_{\mathrm{ws}}^{\star}$ of the washout filter is zero when the input $\Delta\omega$ is constant. The function of the filter is to extract the angular frequency deviation of the power system in the transient state. The time constant τ_{ws} is typically set between 1 and 20 seconds, considering the settling time of the angular frequency deviation [**?**, 12.5].

3.4.2 Phase-lead compensator

The phase-lead compensator is incorporated to alleviate the phase lag from the bus voltage phase to the generator's active power. Typically, one or two phase lead compensators are connected in series to achieve the desired phase lead. Specifically, the dynamic characteristics of the compensator with input v_{ws} from the washout filter is given by:

$$\begin{cases} \tau_{\mathrm{d1}}\dot{\xi}_1 = -\xi_1 + \left(1 - \frac{\tau_{\mathrm{d1}}}{\tau_{\mathrm{n1}}}\right) v_{\mathrm{ws}} \\ v_1 = \frac{\tau_{\mathrm{n1}}}{\tau_{\mathrm{d1}}}(v_{\mathrm{ws}} - \xi_1) \end{cases} \qquad \begin{cases} \tau_{\mathrm{d2}}\dot{\xi}_2 = -\xi_2 + \left(1 - \frac{\tau_{\mathrm{d2}}}{\tau_{\mathrm{n2}}}\right) v_1 \\ v_{\mathrm{pl}} = \frac{\tau_{\mathrm{n2}}}{\tau_{\mathrm{d2}}}(v_1 - \xi_2) \end{cases} \tag{35b}$$

Finally, the output of the power system stabilizer can be obtained by applying the output v_{pl} of the phase-lead compensator to a saturation function:

$$V_{\mathrm{pss}} = \mathsf{sat}\left(v_{\mathrm{pl}}; V_{\mathrm{pss}}^{\mathrm{min}}, V_{\mathrm{pss}}^{\mathrm{max}}\right) \tag{35c}$$

An example of the parameters for this model is shown in Table 7. However, it should be noted that the parameters for the power system stabilizer need to be determined by considering various factors such as the dynamic characteristics of each generator, automatic voltage regulator, load distribution, and characteristics of the transmission network, and that the desired system stability may not necessarily be achieved by the parameter settings shown in the example. In addition, the standard design guidelines for power system stabilizers are often based on the one-machine infinite-bus system model explained in Section **??**, and caution is required regarding the results when multiple generators are interconnected. For example, in [**?**, Section 12.5], design guidelines for parameters based on classical control theory using the one-machine infinite-bus system model are presented. In [**?**], design guidelines based on modern control theory are also explained.

Table 7 IEEE PSS1 type model parameter example

	k_{pss}	τ_{ws}	τ_{d1}	τ_{n1}	τ_{d2}	τ_{n2}	$V_{\mathrm{pss}}^{\mathrm{min}}$	$V_{\mathrm{pss}}^{\mathrm{min}}$
Example 1 [**?**, Section 12.5]	9.50	1.4	0.033	0.154	0.00	0.00	$-\infty$	∞
Example 2 [**?**, Section 12.8]	20.0	10.0	0.02	0.05	5.40	3.00	$-\infty$	∞
Example 3 [**?**, Section III]	1.57	10.0	0.03	0.34	0.03	0.34	$-\infty$	∞
Example 4 [**?**, Table H.3]	3.15	10.0	0.01	0.76	0.01	0.76	−0.09	0.09

3.5 Control Effect of Power System Stabilization Device

Let's analyze the control effect of the power system stabilization device using a simple power system model.

Example 1.5 Changes in the small signal stability and the transient stability due to PSS

Let us consider incorporating a power system stabilization device into the system along with an automatic voltage regulator under the same conditions as Example 1.4. The power system stabilization devices installed in generators 1 and 3 are identical,

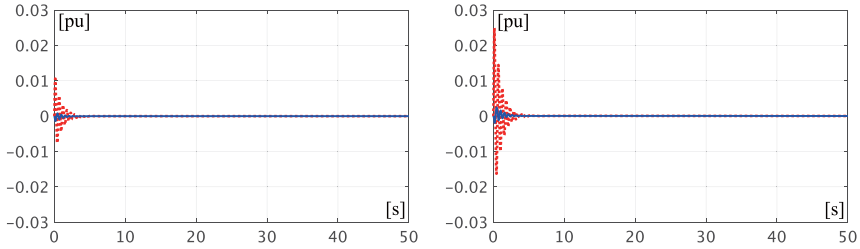

(a) $\delta_1(0) - \delta_3(0) = -1$ (b) $\delta_1(0) - \delta_3(0) = -1.57$

Fig. 12 Initial value response of angular frequency deviation
(There is a system stabilizer, and the line type is the same as **??**)

and the parameters use the values of Example 2 in Table 7. First, let us confirm the change in the set of stable equilibrium points due to the presence of the power system stabilization device, which is shown in the range of (iii) in Table 6. From this result, it can be seen that the set of stable equilibrium points has expanded by incorporating the power system stabilization device.

---

4 PSS based on the retrofit control theory

4.1 Power system model used in the design of PSS

4.1.1 Features of PSS based on the retrofit control theory

In this section, we describe the design methodology of the power system stabilizer based on retrofit control theory [**?**,**?**,**?**,**?**,**?**]. The power system stabilizer designed using this methodology can maintain the steady-state power flow condition in a stable manner even when multiple generators are simultaneously incorporated. In particular, each power system stabilizer has the following features:

- Distributed design is possible with just a mathematical model of generators and AVR that incorporates it.
- Distributed implementation is possible with just the local measurement signal of the voltage phasor and current phasor of generator buses.

Next, we consider the case where the IEEE ST1 type AVR model in Equation 32 is incorporated into the generator model in Equation 29. However, for the sake of simplicity, we exclude saturation of the AVR. Note that the same discussion applies not only to the case with saturation but also to the case where other types of AVRs

are incorporated, the case where existing power system stabilizers are incorporated, and the case where a more detailed generator model is used.

4.1.2 Localized linear subsystem

By designing the interaction inputs appropriately, we consider representing the local subsystem, which is coupled with an AVR of the target generator, as a linear system in the form of:

$$G : \begin{cases} \dot{x} = Ax + Bu + Lv \\ w = \Gamma x \\ y = Cx \end{cases} \tag{36}$$

where the state vector x is a concatenation of the states of the generator model δ, $\Delta\omega$, E, and the AVR model V_{tr}.

In addition, the input u represents the output V_{pss} of the PSS, and the input-output interactions v and w are defined as:

$$v := \begin{bmatrix} P_{\mathrm{mech}} - \frac{E|\boldsymbol{V}|}{X'} \sin(\delta - \angle \boldsymbol{V}) \\ k_{\mathrm{ap}} V_{\mathrm{ref}}^{\star} + \left(\frac{X}{X'} - 1\right) |\boldsymbol{V}| \cos(\delta - \angle \boldsymbol{V}) \\ |\boldsymbol{V}| \end{bmatrix}, \qquad w := \begin{bmatrix} \delta \\ \Delta\omega \\ E \end{bmatrix} \tag{37}$$

Note that the interaction input v in Equation 37 contains the non-linear terms of the generator and the variables of the bus voltage phase. It should be noted that the system matrix in Equation 36 is defined in accordance with the definitions of these signals as follows:

$$\begin{aligned} A &:= \begin{bmatrix} 0 & \omega_0 & 0 & 0 \\ 0 & -\frac{D}{M} & 0 & 0 \\ 0 & 0 & -\frac{X}{\tau X'} & -\frac{k_{\mathrm{ap}}}{\tau} \\ 0 & 0 & 0 & -\frac{1}{\tau_{\mathrm{tr}}} \end{bmatrix}, \quad B := \begin{bmatrix} 0 \\ 0 \\ \frac{k_{\mathrm{ap}}}{\tau} \\ 0 \end{bmatrix}, \quad C := I \\ L &:= \begin{bmatrix} 0 & 0 & 0 \\ \frac{1}{M} & 0 & 0 \\ 0 & \frac{1}{\tau} & 0 \\ 0 & 0 & \frac{1}{\tau_{\mathrm{tr}}} \end{bmatrix}, \quad \Gamma := \begin{bmatrix} 1 & 0 & 0 & 0 \\ 0 & 1 & 0 & 0 \\ 0 & 0 & 1 & 0 \end{bmatrix} \end{aligned} \tag{38}$$

The G in Equation 36 is called a **local linear subsystem**. It should be noted that the nonlinear terms of the generator and the variables of the bus voltage phase are included in the interaction input v in Equation 37. The system matrix of Equation 38 is defined for the local linear subsystem. The model parameters of the local linear subsystem, i.e., the system matrix parameters in Equation 38, are assumed to be known and available for the design and implementation of the power system stabilizer.

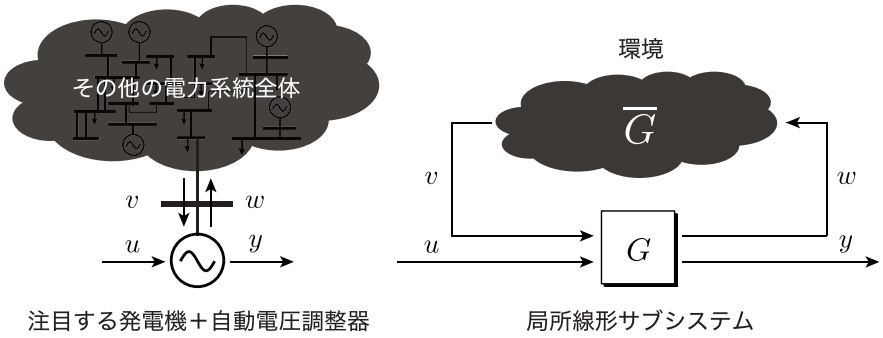

Fig. 13 Coupling system of local linear subsystem and environment

4.1.3 Environment and approximate linear environment model

Let us consider designing a local controller K for the power system stabilization device, under the assumption that the output y and interaction input/output v and w are measurable.

$$K : (y, v, w) \mapsto u$$

In the following, we call this controller K a **retrofit controller**, which derives from the words retroactive and refit and refers to performing partial expansion or reconstruction of an existing system.

In designing and implementing the retrofit controller, not only the model of the local linear subsystem G is used, but also a linear model that estimates the interaction input v from the interaction output w is utilized. We call this estimation model an **approximate linear environment model**.

To explain the approximate linear environment model, we introduce a nonlinear subsystem called the **environment** , which represents the global subsystem of the entire system except for the local linear subsystem. The environment is a nonlinear system that takes the interaction output w of the local linear subsystem as input and outputs the interaction input v. Formally, we represent the dynamic input-output relationship of the environment as:

$$\overline{G} : w \mapsto v$$

In this case, the feedback coupling system between the local linear subsystem G and the environment $\overline{G}$ represents the entire power system from the perspective of the generator under consideration, as shown in Figure 13.

Considering that the environment $\overline{G}$ includes numerous elements such as power transmission networks, loads, and other generators, it is not practical to assume that the complete nonlinear model of the environment is available for the design and implementation of a system stabilizing device for a specific generator. Taking this fact

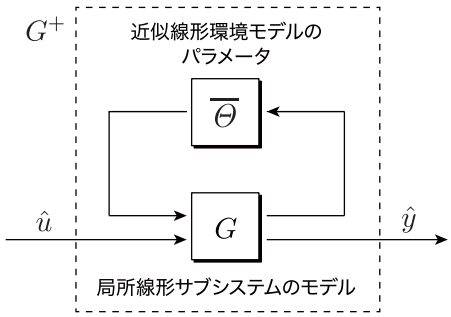

Fig. 14 Model used for controller design

into consideration, let us assume a situation where only an approximate linear model of the environment is available. For simplicity, we will describe the approximate linear environment model using a static input-output relationship. However, it is also possible to use a dynamic approximate linear environment model. For further details, please refer to [**?**].

When the steady-state values of the input-output interaction in the steady-state power flow state of interest are denoted as $(v^\star, w^\star)$, the approximated linearized environmental model is parameterized as follows:

$$\overline{G}_{\text{apx}} : v_{\text{apx}} = v^\star + \overline{\Theta}\left(w - w^\star\right) \tag{39}$$

Here, $\overline{\Theta}$ is a matrix representing the parameters of the model. The approximated linearized environmental model $\overline{G}_{\text{apx}}$ in Equation 39 generates the predicted value v_{apx} of the impact of the interaction output w on the interaction input v in the vicinity of their steady-state values $(v^\star, w^\star)$ by linear prediction.

The power system model used for retrofit controller design is constructed by feedback coupling the parameters of this approximated linearized environmental model $\overline{\Theta}$ with the model of a local linear subsystem G as shown in Figure 14. Specifically, it is given by:

$$G^+ : \begin{aligned} \dot{\hat{\xi}} &= \left(A + L\overline{\Theta}\Gamma\right)\hat{\xi} + B\hat{u} \\ \hat{y} &= C\hat{\xi} \end{aligned} \tag{40}$$

Here, $\hat{u}$ and $\hat{y}$ are virtual input-output signals used for controller design, and are distinguished from u and y by the use of a hat symbol. Note that since C is the identity matrix in Equation 38, the output $\hat{y}$ is equal to the internal state $\hat{\xi}$ of G^+.

4.2 PSS design based on the retrofit control theory

4.2.1 Design method of retrofit controller

Assuming that the approximate linear environment parameter $\overline{\Theta}$ in Equation 39 is identified by an appropriate method, we explain the design method of the retrofit controller. The specific construction method of the approximate linear environment model is described in the next section.

The design of the retrofit controller corresponding to the system stabilization device can utilize the standard control system design method in the field of system control engineering. For instance, let us apply the design method of the **Linear Quadratic Regulator** (LQR) [**?**, Section 5.3] to the controller design model G^+ in Equation 40. In LQR, we use a state-feedback form control algorithm that minimizes the cost function on state and input as follows:

$$J(\hat{\xi}, \hat{u}) := \int_0^\infty \left(\hat{\xi}^\mathsf{T}(t) Q \hat{\xi}(t) + \hat{u}^\mathsf{T}(t) R \hat{u}(t) \right) dt$$

Using the state feedback form in equation 41:

$$\hat{u} = \underbrace{-R^{-1} B^\mathsf{T} P(\overline{\Theta})}_{\hat{K}(\overline{\Theta})} \hat{\xi} \tag{41}$$

Here, Q is a semi-positive definite matrix, R is a positive definite matrix, and the matrix $P(\overline{\Theta})$ satisfies the **Algebraic Riccati Equation** as follows:

$$\left(A + L\overline{\Theta}\Gamma \right)^\mathsf{T} P + P \left(A + L\overline{\Theta}\Gamma \right) - PBR^{-1}B^\mathsf{T}P + Q = 0$$

This equation has a positive definite solution. Then, using the gain matrix $\hat{K}(\overline{\Theta})$ in Equation 41, the retrofit controller is constructed as follows:

$$K : \begin{array}{l} \dot{\hat{x}} = A\hat{x} + L \left\{ v - \overline{\Theta}(w - \Gamma\hat{x}) \right\} \\ u = \hat{K}(\overline{\Theta})(y - C\hat{x}) \end{array} \tag{42}$$

Based on this retrofit control theory, the system stabilization device has the following characteristics for any matrix $\overline{\Theta}$:

- When the power system is in steady-state, the input u becomes zero.
- The stability of the steady-state (equilibrium point) does not change before and after implementation.

The first item means that the retrofit controller does not change the steady-state condition, while the second item means that the implementation of the retrofit controller does not change an asymptotically stable equilibrium point to an unstable one. The objective of retrofit control theory is to improve stability while maintaining the asymptotic stability of the equilibrium point and using indicators such as robustness

to disturbances and the size of the stability region. Note that this method cannot asymptotically stabilize an unstable equilibrium point before controller implementation.

Furthermore, it has been shown that the larger the predictive accuracy of the interaction signal by the approximate linear environmental model, the greater the improvement in system stability. Note that if the control algorithm in equation 41 stabilizes G^+ in equation 40, it is not necessary to use the linear quadratic regulator (LQR) method introduced in section 5.3 of [**?**]. Additionally, $\hat{K}(\overline{\Theta})$ can be a dynamic control algorithm, and it does not need to be static [**?**].

4.2.2 Construction method of approximate linear environmental model

One practical approach for identifying the parameter $\overline{\Theta}$ in Equation 39 is to estimate the relationship between the signals w and v using linearization. Specifically, the partial derivatives of v with respect to each element of w are calculated as:

$$\begin{aligned}
\frac{\partial v}{\partial \delta} &= \begin{bmatrix} -\frac{E|\boldsymbol{V}|}{X'}\cos(\delta - \angle \boldsymbol{V}) \\ -\left(\frac{X}{X'} - 1\right)|\boldsymbol{V}|\sin(\delta - \angle \boldsymbol{V}) \\ 0 \end{bmatrix}, \qquad \frac{\partial v}{\partial \Delta\omega} = \begin{bmatrix} 0 \\ 0 \\ 0 \end{bmatrix} \\
\frac{\partial v}{\partial E} &= \begin{bmatrix} -\frac{|\boldsymbol{V}|}{X'}\sin(\delta - \angle \boldsymbol{V}) \\ 0 \\ 0 \end{bmatrix}
\end{aligned} \tag{43}$$

Therefore, assuming that the internal state of the generator and the voltage phase of the generator bus are in the vicinity of the steady-state conditions, we obtain:

$$\overline{\Theta}^{\text{int}} := \begin{bmatrix} -\frac{E^\star|\boldsymbol{V}^\star|}{X'}\cos(\delta^\star - \angle \boldsymbol{V}^\star) & 0 & -\frac{|\boldsymbol{V}^\star|}{X'}\sin(\delta^\star - \angle \boldsymbol{V}^\star) \\ -\left(\frac{X}{X'} - 1\right)|\boldsymbol{V}^\star|\sin(\delta^\star - \angle \boldsymbol{V}^\star) & 0 & 0 \\ 0 & 0 & 0 \end{bmatrix} \tag{44}$$

Here, the steady-state values of the internal state $(\delta^\star, E^\star)$ of the generator and the steady-state value of the bus voltage phase $(|\boldsymbol{V}^\star|, \angle \boldsymbol{V}^\star)$ are the same as those of $(v^\star, w^\star)$ in Equation 39 under the steady-state conditions. By using the matrix $\overline{\Theta}^{\text{int}}$ in Equation 44, we can model the "local feedback structure that the internal state of the generator itself exerts". Since the normal power system is operated in the vicinity of the steady-state conditions, the steady-state values required for modeling can be identified based on measured data.

Next, let's consider estimating the indirect effect that signal w has on signal v through automatic generation control. The partial derivative of v with respect to the input P_{mech} of automatic generation control is given by:

$$\frac{\partial v}{\partial P_{\text{mech}}} = \begin{bmatrix} 1 \\ 0 \\ 0 \end{bmatrix}$$

When the broadcast-type PI controller in Equation 4 is incorporated as automatic generation control, the time integral of $\omega_0 \Delta\omega$ corresponds to δ, so we have:

$$\frac{\partial P_{\text{mech}}}{\partial \delta} = -\frac{\alpha\beta k_{\text{I}}}{\omega_0}, \qquad \frac{\partial P_{\text{mech}}}{\partial \Delta\omega} = -\alpha\beta k_{\text{P}}, \qquad \frac{\partial P_{\text{mech}}}{\partial E} = 0$$

Therefore, by the chain rule of differentiation, the effect of signal w on signal v through the broadcast-type PI controller can be modeled as:

$$\overline{\boldsymbol{\Theta}}^{\text{agc}} := -\alpha\beta \begin{bmatrix} \frac{k_{\text{I}}}{\omega_0} & k_{\text{P}} & 0 \\ 0 & 0 & 0 \\ 0 & 0 & 0 \end{bmatrix} \tag{45}$$

Note that to obtain this parameter, it is necessary to obtain the values of the controller gains for automatic generation control through an appropriate method.

Similarly, let us consider estimating the indirect effect of signal w on signal v through the bus voltage phasor $\boldsymbol{V}$. The partial derivatives of v with respect to the voltage phasor variables $(|\boldsymbol{V}|, \angle\boldsymbol{V})$ are given by:

$$\begin{aligned} \frac{\partial v}{\partial |\boldsymbol{V}|} &= \begin{bmatrix} -\frac{E}{X'} \sin(\delta - \angle\boldsymbol{V}) \\ \left(\frac{X}{X'} - 1\right) \cos(\delta - \angle\boldsymbol{V}) \\ 1 \end{bmatrix} \\ \frac{\partial v}{\partial \angle\boldsymbol{V}} &= \begin{bmatrix} \frac{E|\boldsymbol{V}|}{X'} \cos(\delta - \angle\boldsymbol{V}) \\ \left(\frac{X}{X'} - 1\right) |\boldsymbol{V}| \sin(\delta - \angle\boldsymbol{V}) \\ 0 \end{bmatrix} \end{aligned} \tag{46}$$

On the other hand, as analyzed in Section **??**, the bus voltage phase not only depends on the internal state of the connected generator but also on the internal states of all other generators. Specifically, let $\overline{\delta}$ and $\overline{E}$ denote the vector of internal states of all generators except the one of interest. Then, the four partial derivatives $\frac{\partial |\boldsymbol{V}|}{\partial \delta}$, $\frac{\partial \angle\boldsymbol{V}}{\partial \delta}$, $\frac{\partial |\boldsymbol{V}|}{\partial E}$, and $\frac{\partial \angle\boldsymbol{V}}{\partial E}$ depend on the vector $z_{\mathbb{G}}$ that combines the internal states of all generators as:

$$z_{\mathbb{G}} := (\delta, \overline{\delta}, E, \overline{E})$$

While it is difficult to obtain analytical expressions for these partial derivatives for general power system models, if we can measure the numerical values of the following matrix in the neighborhood of the steady-state power flow $z^{\star}_{\mathbb{G}}$ using measurement data:

$$\theta := \begin{bmatrix} \frac{\partial |\boldsymbol{V}|}{\partial \delta}(z^{\star}_{\mathbb{G}}) & 0 & \frac{\partial |\boldsymbol{V}|}{\partial E}(z^{\star}_{\mathbb{G}}) \\ \frac{\partial \angle\boldsymbol{V}}{\partial \delta}(z^{\star}_{\mathbb{G}}) & 0 & \frac{\partial \angle\boldsymbol{V}}{\partial E}(z^{\star}_{\mathbb{G}}) \end{bmatrix} \tag{47}$$

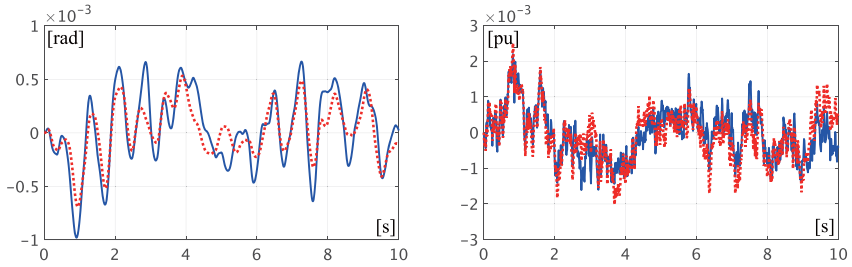

(a) Time series data of δ_3 and $\hat{\delta}_3$

(b) Time series data of E_3 and $\hat{E}_3$

Fig. 15 Time response to random excitation input
(Blue solid line: δ_3, E_3, Red dashed line: $\hat{\delta}_3$, $\hat{E}_3$)

then we can model the indirect effect of signal w on signal v through the bus voltage phase $\boldsymbol{V}$ as:

$$\overline{\Theta}^{\text{ext}} := \begin{bmatrix} -\frac{E^\star}{X'}\sin(\delta^\star - \angle \boldsymbol{V}^\star) & \frac{E^\star|\boldsymbol{V}^\star|}{X'}\cos(\delta^\star - \angle \boldsymbol{V}^\star) \\ \left(\frac{X}{X'} - 1\right)\cos(\delta^\star - \angle \boldsymbol{V}^\star) & \left(\frac{X}{X'} - 1\right)|\boldsymbol{V}^\star|\sin(\delta^\star - \angle \boldsymbol{V}^\star) \\ 1 & 0 \end{bmatrix} \hat{\theta} \tag{48}$$

where $z^\star_{\mathbb{G}}$ in Equation 47 denotes the steady-state value of $z_{\mathbb{G}}$.

The 0 element in the second column corresponds to $\frac{\partial|\boldsymbol{V}|}{\partial\Delta\omega}$ and $\frac{\partial\angle\boldsymbol{V}}{\partial\Delta\omega}$. Furthermore, $\hat{\theta}$ in Equation 48 represents the identified value of θ. $\overline{\Theta}^{\text{ext}}$ in Equation 48 models the "global feedback structure that the internal state of the generator exerts on itself," in contrast to $\overline{\Theta}^{\text{int}}$ in Equation 44, which models the local feedback structure.

It is necessary to identify the parameter $\hat{\theta}$ using data measured during operation, as the power system must always be operated stably. In control engineering, identifying subsystems within an operating feedback system is called "closed-loop identification" [**?**]. Closed-loop identification is often more difficult than identification when input excitation is possible, as it is generally not possible to freely excite the input of the system being identified.

When using all the estimates obtained from the aforementioned linearization approximations simultaneously, the model parameters in Equation 39 are composed of:

$$\overline{\Theta} = \overline{\Theta}^{\text{int}} + \overline{\Theta}^{\text{agc}} + \overline{\Theta}^{\text{ext}} \tag{49}$$

As previously explained, the retrofit controller in Equation 42 does not change the stability of the steady-state power flow for any matrix $\overline{\Theta}$. However, to maintain the predicted accuracy of the interaction signals obtained from the linearized environment model, it is desirable to update $\overline{\Theta}$ at appropriate intervals to respond to changes in the power flow state.

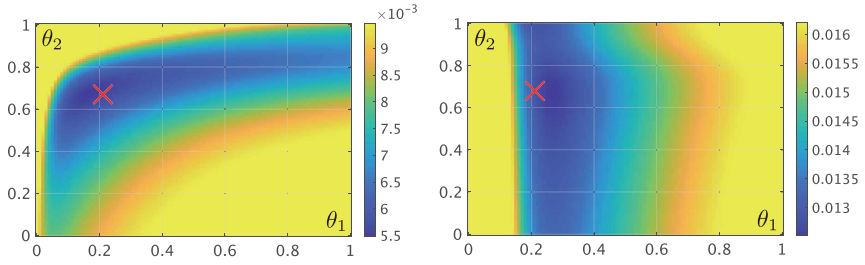

(a) $Q(\delta_3, \hat{\delta}_3)$ (b) $Q(E_3, \hat{E}_3)$

Fig. 16 Approximation error of internal state with respect to identification parameter

Example 1.6 Identification of approximate linear environment model based on measurement data

Similar to Example 1.4, we consider a power system model consisting of three buses, with the same AVR incorporated into generators 1 and 3. We also assume that a broadcast-type PI controller with parameter values given in Table 1(b) is incorporated as automatic generation control according to Equation (4). The steady-state power flow condition corresponds to the results of the power flow calculation in Table **??**.

In the following, we focus on generator 3 and identify the values of partial derivatives of θ_3 in Equation 47 from measurement data. However, the magnitudes of $\frac{\partial |\boldsymbol{V}3|}{\partial \delta_3}(z\mathbb{G}^\star)$ and $\frac{\partial \angle \boldsymbol{V}3}{\partial E_3}(z\mathbb{G}^\star)$ are relatively small, so we identify only two values of θ_1 and θ_2 from the data, where:

$$\theta_1 := \frac{\partial |\boldsymbol{V}_3|}{\partial E_3}(z_{\mathbb{G}}^\star), \qquad \theta_2 := \frac{\partial \angle \boldsymbol{V}_3}{\partial \delta_3}(z_{\mathbb{G}}^\star)$$

At this time, $\overline{\boldsymbol{\Theta}}_3^{\text{ext}}$ in Equation 48 is parameterized as:

$$\overline{\boldsymbol{\Theta}}_3^{\text{ext}} = \begin{bmatrix} \frac{E_3^\star |\boldsymbol{V}_3^\star|}{X_3'} \Delta_3^{\cos} \theta_2 & 0 & -\frac{E_3^\star}{X_3'} \Delta_3^{\sin} \theta_1 \\ \left(\frac{X_3}{X_3'} - 1\right) |\boldsymbol{V}_3^\star| \Delta_3^{\sin} \theta_2 & 0 & \left(\frac{X_3}{X_3'} - 1\right) \Delta_3^{\cos} \theta_1 \\ 0 & 0 & \theta_1 \end{bmatrix} \tag{50}$$

where $\Delta_3^{\sin}$ and $\Delta_3^{\cos}$ are constants defined by:

$$\Delta_3^{\sin} := \sin(\delta_3^\star - \angle \boldsymbol{V}_3^\star), \qquad \Delta_3^{\cos} := \cos(\delta_3^\star - \angle \boldsymbol{V}_3^\star)$$

The optimization of the parameters (θ_1, θ_2) is carried out using the following procedure. Time series data of (δ_3, E_3) obtained by randomly exciting the input $V_{\text{pss}3}$ of the AVR is obtained from the power system model. Furthermore, a controller design model G_3^+ for the feedback system of the local linear subsystem G_3 and the approximate linear environmental model parameters $\overline{\boldsymbol{\Theta}}_3$ of Equation 36 is constructed for

generator 3 using Equation 40. Here, $\overline{\Theta}_3$ is defined by Equation 49. Then, time series data of $(\hat{\delta}_3, \hat{E}_3)$ are obtained as the first and third elements of $\hat{y}3$ when the signal used to excite Vpss3 is applied as the input $\hat{u}_3$ of Equation 40. The parameters (θ_1, θ_2) are optimized such that for all time instants t in the time interval where the data is obtained, $\hat{\delta}_3(t)$ and $\hat{E}_3(t)$ are good approximations of $\delta_3(t)$ and $E_3(t)$, respectively.

The time series data of (δ_3, E_3) is shown for the period from 0 [s] to 10 [s] when V_{pss3} is randomly excited, as indicated by the blue line in Figure 15. However, the deviations from the steady-state values $(\delta_3^\star, E_3^\star)$ are also shown. The results of an exhaustive search for the optimal parameters (θ_1, θ_2) on an evenly spaced grid with a width of 0.01 for this data are shown in Figure 16. The horizontal and vertical axes represent the values set for θ_1 and θ_2, respectively, and the colors in regions (a) and (b) represent the values of the error functions $Q(\delta_3, \hat{\delta}_3)$ and $Q(E_3, \hat{E}_3)$, respectively.

Here, the error function $Q(x, \hat{x})$ is defined as follows:

$$Q(x, \hat{x}) := \sum_{k=1}^{1000} \left\| x\left(\frac{k}{100}\right) - \hat{x}\left(\frac{k}{100}\right) \right\|^2$$

It evaluates the error of the continuous-time signal $x(t)$ for $t \in [0, 10]$ with respect to the discrete-time signal $\hat{x}(t)$ sampled at 1,000 points with a period of 0.01 [s].

Based on these results, the parameter values are set to $(0.215, 0.675)$. Note that this parameter value corresponds to the "x" mark in Figure 16. The time series data of $(\hat{\delta}_3, \hat{E}_3)$ for this parameter setting is shown as the red dashed line in Figure 15. It can be seen that the behavior of the internal state of generator 3 is captured by the obtained approximate linear environment model.

In Example 1.6, the parameters of the approximate linear environment model are identified as the index of the precision by which the internal state of the generators is approximated. The effect of the retrofit control based on this identification method is presented in Chapter **??**.